EXPERIMENAL AND NUMERICAL INVESTIGATION OF THERMAL STRATIFICATION DURING VENTING ON A CRYOGENIC STORAGE TANK

A PROJECT REPORT

submitted by

ROHITH S

REG. No: TKM20MEIR13

to

The APJ Abdul Kalam Technological University
in partial fulfilment of the requirements for the award of the Degree of
Master of Technology

in

Industrial Refrigeration and Cryogenic Engineering

DEPARTMENT OF MECHANICAL ENGINEERING

T K M College of Engineering, Kollam

AUGUST 2022

DEPARTMENT OF MECHANICAL ENGINEERING T.K.M COLLEGE OF ENGINEERING, KOLLAM

CERTIFICATE

This is to certify that the report entitled "***Experimental and Numerical Investigation of Thermal Stratification During Venting on a Cryogenic Storage Tank***" submitted by **ROHITH S**, Reg. No: **TKM20MEIR13** during **2020-2022** to the APJ Abdul Kalam Technological University in partial fulfillment of the requirements for the award of the Degree of Master of Technology in Industrial Refrigeration and Cryogenics Engineering, Department of Mechanical Engineering is a bonafide record of the project work carried out by him under our guidance and supervision.

Project Guide:
Dr. Vishnu S.B.
Assistant Professor
Dept. of Mechanical Engineering
T K M College of Engineering, Kollam

PG Coordinator:
Dr. K.A. Shafi,
Professor
Dept. of Mechanical Engineering
T K M College of Engineering, Kollam

Dr. P.N Dileep
Proffessor & Head
Dept. of Mechanical Engineering
T K M College of Engineering, Kollam

DECLARATION

I, Rohith S, hereby declare that this project report entitled "**Experimental and Numerical Investigation of Thermal Stratification During Venting on a Cryogenic Storage Tank**", submitted for partial fulfilment of the requirements for the award of degree of Master of Technology of the APJ Abdul Kalam Technological University, Kerala is a bonafide work done by me under supervision of Dr.Vishnu.S.B, Assistant professor, T K M College of Engineering Kollam. This submission represents my ideas in my own words and where ideas or words of others have been included, I have adequately and accurately cited and referenced the original sources. I also declare that I have adhered to ethics of academic honesty and integrity and have not misrepresented or fabricated any data or idea or fact or source in my submission. I understand that any violation of the above will be a cause for disciplinary action by the institute and/or the University and can also evoke penal action from the sources which have thus not been properly cited or from whom proper permission has not been obtained. This report has not been previously formed the basis for the award of any degree, diploma or similar title of any other University.

Rohith S

Reg.No: TKM20MEIR13 of the year 2020-2022

Dr. Vishnu S.B.
Assistant Professor
Dept. of Mechanical Engineering
T K M College of Engineering, Kollam

Dr. P.N. Dileep,
Head of the Department
Dept. of Mechanical Engineering
T K M College of Engineering, Kollam

31/08/2022

ACKNOWLEDGEMENT

I take this opportunity to express my deep sense of gratitude and sincere thanks to all who helped me to complete the project successfully.

Firstly, I would like to express my heartfelt thanks to my guide **Dr. Vishnu S.B,** Assistant Professor, Department of Mechanical Engineering for his selfless support, guidance, motivation, great encouragement, and valuable comments during the course of project and during the preparation of this report.

I am extremely thankful to **Dr. T.A. Shahul Hameed,** Principal TKM College of Engineering for providing excellent experimental facilities at TKM Engineering College from bottom of my heart for lending me all facilities and support for the completion of project.

I express my gratefulness to my PG coordinator **Dr. K.A Shafi**, Professor, Department of Mechanical Engineering and **Dr. P.N. Dileep**, Professor & Head of Department, Mechanical Engineering for rendering their valuable suggestions, timely advice, and support throughout the work.

I express my deep sense of gratitude to thank **Dr. Mohammed Sajid N.K**., Professor and former Head of Department and **Dr. Mohammed Sadhikh**, Professor, former PG Co-ordinator, Department of Mechanical Engineering, TKM College of Engineering from bottom of heart for the support they have rendered during my project.

I thank **Dr. Krishnakumar,** Department of Mechanical Engineering for allowing me to conduct my experimental procedure in Nano Technology lab.

I also mark my deep gratitude to all the faculty of Department of Mechanical Engineering and my beloved classmates for their support and constructive intervention.

Rohith S

ABSTRACT

Over the years, the need for exact estimation and comprehension of thermal stratification and self-pressurization in a cryogenic storage has grown, as the stratification phenomenon is dependent on the architecture of the cryogenic storage. The cryogenic engines use liquid fuels that are stored in liquid form at extremely low temperatures. Since propellants are stored at their boiling temperature or subcooled condition, small heat infiltration can cause thermal stratification and self-pressurization. When heat is transferred to the propellent tank, the liquid near to the side wall is heated up, and a boundary layer will develop. The warm fluid inside the boundary layer will move upwards and is dumped at the liquid-vapor interface. The warm fluid layer developed at the liquid-vapor interface is known as a thermally stratified layer, and this phenomenon is known as thermal stratification. Experiments are carried out to examine the effects of self-pressurization and temperature stratification on cryogenic storage tanks in order to avoid stratification. As a result, the current research work aimed to improve the understanding of the combination of thermodynamics, fluid dynamics and combined heat transfer phenomena of cryogenic propellant tank pressurization, thermal stratification. An experimental setup was developed to study the stratification. A cryogenic storage tank with foam insulation has been designed, fabricated, and used for the stratification studies, using liquid nitrogen. To support the experimental findings, a numerical analysis was done using the ANSYS FLUENT software. The model is validated with the experimental result. The Volume of Fluid (VOF) method is used to predict the liquid-vapour interface movement.

Keywords: Thermal stratification, self-pressurization, venting, non-venting, cryogenic tank.

CONTENTS

LIST OF TABLES

LIST OF FIGURES

ABBREVATIONS

CFD	Computational Fluid Dynamics
FDM	Finite Difference Method
FEM	Finite Element Method
FVM	Finite Volume Method
TC	Thermo-Couple
DAQ	Data Acquisition System

CHAPTER 1

INTRODUCTION

Thermal stratification is a crucial component of designing cryogenic tanks because it can have a big influence on the rate of pressurization. Liquid hydrogen and oxygen serve as the fuel and oxidizer in cryogenic engines, respectively. Natural convection currents are produced by raising the liquid temperature close to the wall as a result of heat seeping. This phenomenon causes the fuel condition inside the tank to change, hence it's crucial to maintain the propellant qualities in the predetermined state.

Fuel utilization in liquid hydrogen-fueled rocket vehicles becomes a major problem since liquid hydrogen has a tendency to thermally stratify at a layer near to the liquid vapour interface. The launch vehicle will likely be destroyed if warm propellant from this layer is delivered to the rocket propellant feed system due to cavitation.

The goal of this work is to figure out what causes thermal stratification at high pressure and during the venting-off phase. Also, it's important to build a small cryogenic vessel and do experiments with liquid nitrogen to learn more about the thermodynamics and fluid dynamics of thermal stratification during the vent-off period in a cryogenic storage tank and find a way to get rid of it.

1.1 APPLICATIONS OF CRYOGENICS

Cryogenic technologies are widely used in a wide range of applications.

a) Cryogenic propulsion

Fuels that must be kept in liquid form at cryogenic temperatures and in gaseous form at room temperature are used in cryogenic engines. The most used cryogenic propellant combination is liquid hydrogen (fuel) and liquid oxygen (oxidizer). Due to the liquid propellant's comparatively high density, a smaller tank size with a higher mass ratio is possible.

b) Transport

The majority of the time, cryogenic fuels are liquefied gases like liquid hydrogen, liquid natural gas, etc. These have been utilised as fuels and propellants for vehicles with IC engines. Storage tanks can accommodate more fuel in the same capacity as compressed gas tanks because cryogenic fuel has a higher energy density than gaseous fuels.

c) Aerospace Applications:

Liquid helium is used to inflate the enormous balloons on airships, and liquid oxygen is utilised onboard as a breathing gas for the pilots. Liquid helium at 4.2 K is stored and transported in specialised cryogenic containers called Heister Dewars, which can endure internal pressures of up to 10 bar. Fighter jets employ argon or nitrogen gas to fill the tyres of the aircraft with nitrogen and to produce an inert atmosphere in the fuel tank.

d) Medical Applications:

Low temperatures have major effects on living tissue that either preserve or destroy life as a result of a decline in activity. When living tissue is exposed to cryogen, it can be instantly destroyed or kept for years without showing any signs of biological activity. Basic understanding of these has resulted in real-world applications for cell destruction and long-term storage (cryopreservation) (Cryosurgery). In order to preserve human or animal dead remains at extremely low temperatures (below 140 K), a process known as cryonics was developed.

e) Food Freezing and Storage:

Liquid nitrogen and cryogen are both frequently utilised for specialised cooling and freezing applications. In blast freezing or immersion freezing systems, liquid nitrogen is required for the freezing of foods like vegetables, fruits, nuts, fish, flowers, and medical products like vaccines. In order to remove heat from products and create an atmosphere with extremely low temperatures, specific cryogenic equipment types are employed.

1.2 PROPELLANTS USED IN CRYOGENICS

there are combinations of fuel and oxidizers, some of them are:

- Liquid oxygen (LOX) and liquid hydrogen (LH2)
- Liquid oxygen (LOX) and kerosene
- Liquid oxygen (LOX) and gasoline
- Hydrogen peroxide and kerosene
- Nitric acid (HNO3) and kerosene
- Liquid oxygen (LOX) and ethanol (C2H5OH)

liquid hydrogen and liquid oxygen are generally used as cryogenic propellants in the high-efficiency main engines of the space shuttle.

1.3 CRYOGENIC TANKS

It is made to withstand internal fluid pressure as well as heat infiltration from the surrounding environment. Aluminium, stainless steel, titanium alloy steel, and fibre reinforced polymers are frequently used for tanks, along with a thin, impermeable inner liner of metal to stop leakage through the fibre reinforced walls' pores. To account for the gases that will change as a result of evaporation, some "ullage" space should be allowed. The volume of ullage typically ranges from 3 to 10% of the tank volume.

1.4 THERMAL STRATIFICATION

The liquid close to the sidewall will warm up as heat is transported to the storage tank, and a boundary layer will form as a result. At the liquid-vapor interface, the warm fluid that is present in the boundary layer will flow upward and be ejected. Thermal stratification is the scientific name for the process whereby a warm fluid layer forms at the liquid-vapor interface. The status of the propellant inside the tank changes as a result of stratification. To restart the cryogenic engine after the coast phase, it is crucial to maintain the propellant qualities in a predetermined condition. The temperature at the liquid-vapor interface rises as a result of stratification, and the internal tank pressure will be at the saturation level that corresponds to the stratum temperature.

Successive venting is necessary to keep the tank pressure within a predetermined range. The period between successive venting must be shortened due to stratification's increased rate of pressurisation, which creates serious issues with cryogen handling and storage. There are further justifications for eliminating thermal stratification. The condition of the propellant at the entrance of the propellant feed system or turbo pump must fall within a specific range for cryogenic rocket engines. The flight vehicle will probably be destroyed by cavitation if the inlet temperature is higher than the cavitation value.

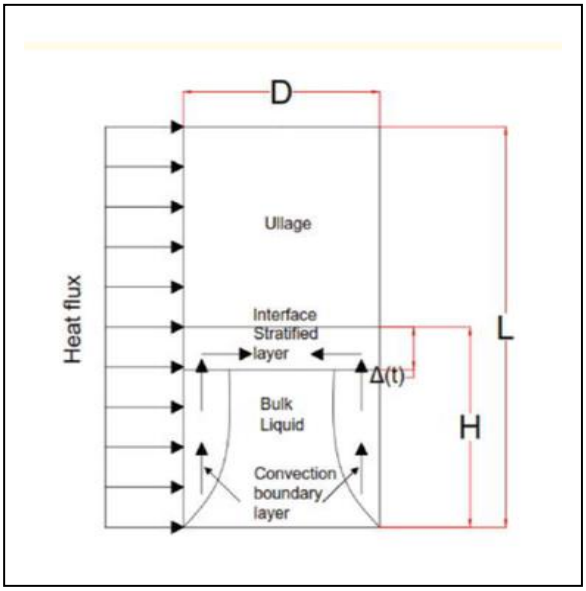

Fig 1.1 Schematic of Thermal Stratification Phenomena

1.5 CAVITATION

When the local pressure drops below the working liquid's saturation pressure, a phenomenon known as cavitation occurs. The liquid oxygen and hydrogen are drawn from their respective tanks by the cryopumps, which then discharge them at high pressure into the combustion chamber for mixing and combustion. The system may experience cavitation because of the very high rotational speed of these pumps.

1.6 OBJECTIVES OF THE RESEARCH

By studying thermal stratification at high pressures and during vent off periods, the current research work hopes to better understand the thermodynamic and fluid dynamic phenomena of a cryogenic storage tank.

1. Conducting an extensive literature survey to understand the thermal stratification phenomena in a cryogenic storage tank and its importance in cryogenic applications.
2. Design and develop a cryogenic storage vessel with foam insulation to study the evolution of stratification.
3. Conduct experimental investigation on the storage tank with liquid nitrogen as model propellant.
4. Figure out various factors affecting the stratification phenomena in a cryogenic storage tank.
5. Study of stratification at elevated pressure and during vent off period.
6. Develop a numerical model using Ansys Fluent to predict the stratification phenomenon of a cryogenic storage tank.
7. Validate the numerical model with the experimental results
8. Study the fluid flow and heat transfer taking place during venting off and its effect on stratification phenomena inside the storage tank.

1.7 THESIS OUTLINE

This thesis involves the experimental and numerical analysis on the thermal stratification phenomenon during venting at elevated pressure. This thesis is presented in seven chapters.

- Chapter 1 provides a brief introduction to cryogenics and applications, the evolution of thermal stratification and self-pressurization.
- Chapter 2 provides details about the historical background, experimental and numerical studies conducted to predict the state of the cryogen inside a storage vessel.
- Chapter 3 provides a brief overview of the Computational Fluid Dynamics.
- Chapter 4 contains the design and development of a cryogenic storage tank with foam insulation, experimental Investigation of the stratification by venting.
- Chapter 5 describes the numerical model developed to predict the self-pressurization and thermal stratification phenomena on a cylindrical cryogenic storage vessel.

- Chapter 6 includes results from experimental and numerical simulation concerning the study of thermal stratification.
- Chapter 7 includes the conclusions derived from the experimentation and numerical analysis performed in association with the present research work.

CHAPTER 2

LITERATURE SURVEY

2.1 STUDIES ON THE EFFECT OF THERMAL STRATIFICATION

Understanding the thermal stratification phenomenon at high pressure and during the vent-off phase is the aim of the current study. In order to comprehend the thermodynamic and fluid dynamic phenomenon of thermal stratification during the vent off period in a cryogenic storage tank and develop a method to reduce the stratification, it is also necessary to build a small-scale cryogenic vessel and conduct experiments using liquid nitrogen. The recent development in the field of thermal stratification have been presented here in this section.

A two-phase CFD model is presented by S. Barsi and M. Kassemi (2008) in their study to characterize the self-pressurization behaviour of a flying weight partially filled LH2 tank in normal gravity. The predictive power of the model is evaluated using historical experimental data at various fill levels, and it was discovered that the predictions show a favourable agreement with the experimentally measured pressure histories. It is proposed that a non-uniform heat load may be the cause of the small variances seen for the median fill level scenarios.

According to Sangeun Roh and Gihun Son (2012), transient natural convection in a pressurised LNG storage tank was calculated by using a commercial CFD code called Fluent to solve the conservation equations for mass, momentum, and energy. The heat balance at the liquid-vapor interface can be used to forecast the rate at which boil-off gas (BOG) will vaporise from the liquid. We study pressurising a storage tank as one of the BOG reduction strategies. The numerical results demonstrate that the vertical temperature distribution, which is impacted by the increasing tank pressure, greatly influences the BOG generation pattern. On the BOG generation pattern, the impacts of tank pressure, tank size, and pressurisation technique are quantified. The heat balance at the liquid-vapor interface served as a basis for estimating the production of boil-off gas (BOG). By raising tank pressure,

the BOG generation rate can be greatly lowered, as shown by the computation presented here. As the pressurisation level and tank capacity increase, the reduction of BOG generation also grows. Additionally, the analysis demonstrates that both progressive and rapid pressurisation can reduce BOG formation. The stored BOG is virtually the same regardless of the pressurisation method.The processes of thermal stratification and de-stratification in liquefied gas tanks with heat leak through the side wall were statistically investigated, according to Jing-Jie Ren and Jian-Yun Shi (2013). The experimental results from the literature were used to validate the calculating model created using ANSYS FLUENT 12.0. At the stratification and de-stratification stages, the liquid flow behaviours and temperature distributions were shown, and their interactions were examined.

They discovered that when a liquid is stratified, the flow field displays a semi circulation close to the liquid top with a plume-like flow beneath it, and there is a cold core beneath the surface that resists the warmer circulating flow. Once the circulation forms and extends downward to make the thermal stratifications disappear layer by layer from up to down, the de-stratification of the stratified liquid starts when the circulating loops close with the resistance reduced due to the disappearance of the cold core. The liquid's flow behaviour affects the thermal stratification and de-stratification, and the temperature distribution has an impact on the flow field. They found that a plume-like flow is present beneath a semi circulation close to the liquid surface when a liquid is stratified. Due to the circulation flow produced by the rising stream close to the heated wall, the liquid surface is at its warmest. The heat is then transferred to the bulk by the downward plume flow. Another aspect of stratification is the presence of a cold core below the surface that opposes the warmer circulation flow. As the liquid temperature rose completely and the temperature stratifications of the liquid engaged in the circulation were eliminated, the resistance to the circulation was lowered due to the elimination of the cold core near the surface. Once finished, the circulation continued to expand downward, causing the implicated thermal stratifications to mix one layer at a time. The temperature of the liquid increased more quickly throughout the destratification process while it was entrained by the circulation, but it increased more slowly after being mixed. The vaporisation spots are situated in

the de-stratification region, which can cause the de stratification to slow down the build-up of pressure.

Juan Fu and Bengt Sunden (2014) conducted an experimental examination to examine the Self-pressurization in a cylindrical ribbed tank that is partially filled with liquid hydrogen quantitatively under various rib spacing-to-height ratios. Both the volume of Fluid (VOF) approach and a phase transition model are used. The computations are performed by the user-defined functions using models that are appropriate for Ansys Fluent. To forecast fluid flow currents and heat transfer, the ribbed surface is represented as a finned surface and a conjugate transient heat transfer problem is developed. Additionally, studied is the impact of rib material and form.

They discovered that mounting ribs on the tank wall can lower the pressure rise. The rib spacing to height ratio decreases, increasing the severity of this condition. When the spacing-to-height ratio is relatively high, a vortex is seen in the area downstream of each rib. As time passes, evaporation happens as a result of heat building up at the rib surfaces. When the ribs have the same arrangement in geometry, pressure rises more slowly with high thermal conductivity ribs and faster with low thermal conductivity ribs. The final pressure rise appears to increase monotonically over time rather than rapidly. In terms of controlling the pressure rise and temperature stratification for the same cross-sectional area and assuming the positions are maintained, semi-circular ribs outperform rectangular ones. Their conclusions include Ribs installed on the wall can improve heat transfer by allowing the heated liquid and bulk liquid to mix more thoroughly before the warm liquid flows up to the interface for evaporation. As a result, both the pressure rises and the degree of thermal stratification decrease. As the rib spacing-to-height ratio is decreased, the rate of pressure rises lowers. When the ratio has a reasonably high value, an eddy is seen at the start port of the upper surface of the ribs.

The rectangular rib's lower and upper surfaces perform in terms of heat transfer less effectively than its top surface. As a result of heat accumulation caused by heat conduction in the rib, evaporation is facilitated and the saturation temperature is only marginally altered by the slower pressure rise. In comparison to high thermal conductivity ribs of the same configuration in geometry, pressure

is higher for low thermal conductivity ribs. The final pressure rise appears to be increasing monotonically with time, and if the positions of the ribs are maintained, semi-circular ribs outperform rectangular ones in terms of controlling pressure rise and temperature stratification for the same cross-sectional area of the ribs.

Using a CFD model, Zhan Liu and Yanzhong Li (2016) looked at the pressurisation performance and thermal stratification in the cryogenic liquid oxygen (LOX) tank that is used in the final stage of a rocket's launch and is exposed to aerodynamic heat and space radiation. Aerodynamic heat and space radiation have both been taken into account through the compilation of one UDF and its implantation into the CFD model through iterative calculation with variable physical properties in each time step. It turns out that aerodynamic heat has had a significant impact on tank pressurisation performance, although space radiation's impact is less clear.

As a result of condensation during active-pressurization, tank pressure, which is influenced by the injection gas, varies between the minimum and maximum pressure limit and the ullage mass decreases. Meanwhile, the temperature distribution's fundamental parallel progress tendency is essentially formed. Tank pressure initially drops quickly during the pressurised discharge, then declines linearly before finally increasing at a faster rate. As the liquid's height decreases, the temperature of the liquid steadily rises in the direction of advancement. The temperature of the remaining liquid also clearly rises. The ullage is continuously condensing during the operation as a result of heat transfer from the ullage to the liquid.

They came to the conclusion that about 60 seconds from the start of the launch, aerodynamic heat flux starts to have a noticeable impact on the tank pressurisation process. In roughly 120 seconds, the aerodynamic heat flux achieves its maximum value of 1654 W/m2. The tank pressure rise interval has been shorter, whereas the tank pressure decline period has gotten longer due to the rising aerodynamic heat flux. The lowest and maximum time intervals for tank pressure increases and decreases, respectively, are 4 s and 13 s, respectively, and are completed in around 120 s. Aerodynamic heat has aided in the pressurisation of the tank, increasing the pressurised time by 9.2 seconds and the pressured gas mass by

1.656 kg when compared to the pressurisation performance calculated in an adiabatic state. Depending on the flight altitude and phase change, the total space radiation flux ranges from 580 W/m2 to 640 W/m2. Due to the rapid pace of fluid loss, its effects are not immediately apparent. Tank pressure varies between the minimum and maximum pressure limits while active pressurisation is in progress. The ullage mass likewise varies and exhibits a general decreasing tendency with the ullage condensation and gas injection. While in the pressurised discharge part, the tank pressure decreases abruptly at first, then linearly, and then has a higher reducing rate. This is due to the tank shape. The ullage mass has an increasing trend accompanied with weak fluctuation change. The liquid mass almost linearly decreases.

Additionally, the ullage is always reduced during the entire process while taking phase change into account. Fluid temperature distribution during active-pressurization is disrupted significantly by the pressured gas, with major disturbances emerging in the ullage and liquid near the interface. However, a general representation of the temperature distribution parallel trend is shown. As liquid height decreases during the pressurised discharge, fluid temperature gradually rises in the direction of advance. The liquid-vapor interface develops better temperature transition. The temperature of the remaining liquid always steadily increases because more heat is transferred from ullage to liquid.

A transient analytical, multi-phase, thermodynamic model of a foam-insulated liquid hydrogen tank has been created, according to Jeswin Joseph and Gagan Agrawal (2016), to better understand the impact of insulation thickness on the evolution of tank pressure and liquid thermal stratification. Experimental data published in the literature are used to validate the model. Two scenarios are taken into account in the analyses for pressurisation: the first case, in which the tank vent port is closed after pressurisation to study the evolution of pressure, and the second case, in which the tank pressure is kept constant at 3.0bar to study the development of liquid thermal stratification.

They learned Both examples are examined with pressurisation gas temperatures of 50K and various tank insulation thicknesses of 10mm, 20mm, 30mm, and 40mm. Analysis is also done on how the self-pressurization profile of

the tank is affected by changes in ambient wind velocity and the presence of solar flux. The study demonstrates that an increase in stratified mass results from a reduction in insulating thickness. When a tank is insulated with thinner insulation, the study also shows a considerable rise in pressure. They discovered that lower insulation thickness over cryogenic tanks causes a larger heat infiltration into ullage gas, which dramatically raises tank pressure. The evolution of the stratified mass is significantly influenced by tank pressure, which affects interface temperature. Higher tank pressure results in more stratified liquid mass. Propeller tanks used in launch vehicles suffer a payload penalty due to increased stratified mass as a result of higher liquid heat infiltration from the environment when tank insulation is thinner. Due to a higher ullage heat in-leak, a lower tank insulation thickness reduces the amount of pressurising mass needed to pressurise the tank. After pressurisation, more ullage mass must be released in order to keep tank pressure constant. The heat in-leak and subsequent tank pressure are influenced by the tank's outer surface temperature, which is determined by surrounding conditions and sun flux.

To understand the initial stages of convective flow phenomena and the ensuing thermal stratification of cryogenic liquid, Sung Woong Choi and Woo Il Lee (2017) performed a numerical study of natural convective flow in a cryogenic tank with a capacity of 4.9 m3 using the liquid-vapor mixture model. To compare their effects, two cryogens—liquefied natural gas (LNG) and liquefied nitrogen (LN2)—were used. They found that s. LN2 exhibited faster vaporisation owing to its lower heat of vaporization. It was observed that higher heat flux and lower filling level led to faster vaporisation and relatively vigorous heat transfer, showing early thermal stratification. The adaptability of the numerical models was validated by existing experimental. They came to the conclusion that circulating currents developed at different periods under various heat flux circumstances. Circulating flow currents formed more quickly under situations of higher heat flux. For various liquid filling level conditions, higher filling levels needed substantially more time for evaporation, whereas low filling level conditions exhibited relatively larger values of stream function. Different degrees of heat flux and the liquid filling level had a significant impact on the pressure rise and pace of growth. Pressure increase and rate of increase grow as heat flux increases and filling level declines.

Early in the LN2 timeline, rather active heat transfer and circulation behaviour occurred in the liquid, indicating that heat transfer into the vapour zone happens more quickly. As a result, LN2 saw a greater pressure rise than LNG. With time of evaporation, it was found that the degree of thermal stratification was weak along the axis of the tank. As the heat flux increased, the degree of thermal stratification in the direction of the liquid's bulk became higher over time. For the low filling level situation near the interface, the thermally stratified layer grew more quickly. Compared to LNG, LN2 experienced early temporal mixing and the transition to thermal stratification more quickly.

M. Xavier and R. Edwin Raj (2017) looked into thermal stratification in a cryogenic propulsion stage's LH2 tank during testing at an ISRO site. In a cryogenic propulsion system, liquid oxygen and hydrogen are employed as the oxidizer and fuel, respectively. These liquids are kept in cryogenic propulsion system tanks that are foam-insulated and pressurised with warm pressurant gas that is provided to maintain tank pressure while the cryogenic engine is running. Warm liquid strata forms at the liquid free surface as a result of buoyancy-driven liquid stratification caused by heat loss to cryogenic propellant tank. By adding warm pressurant gas to the tank during engine operation, this warm stratum is heated even more. It is necessary to model the thermal stratification in order to predict the temperature of the stratified layer and the mass of the stratified liquid in the tank at the conclusion of engine operation because the stratified layer temperature directly affects the cavitation-free operation of the turbo pumps integrated into cryogenic engines. These inputs are necessary to calculate the minimum pressure that the tank pressurisation system must maintain. They outline the layout of the cryogenic stage for the ground qualification test, the stage hot test sequence, a thermal model, and its findings for a foam-insulated LH2 tank that was pressurised with hydrogen gas at 200 K while the liquid was being pumped out at 38 lps for engine operation.

In order to predict the temperature of the liquid stratum and the mass of stratified liquid in the tank at the conclusion of engine operation in stage qualification tests conducted in ISRO facility, the aforementioned model takes into account buoyancy flow in free convection boundary layer caused by heat flux from tank wall and energy transfer from warm pressurant gas, among other factors. They created a mathematical model that describes the formation of thermal stratification

in a liquid hydrogen tank of a cryogenic propulsion system that is powered by natural convection. It takes into account how tank wall heat flux affects the stratified layer, as well as how heated pressurant gas (provided for tank pressure management) transfers heat. To anticipate the temperature of the stratified layer, Ts, and its thickness, temperature and velocity boundary layers at the tank's inner surface are taken into consideration (t). When considering the 38 lps of liquid that are expended during engine operation, the effect of thermal stratification is examined. The model was used to simulate the thermal stratification in a 30 m3 foam-insulated LH2 tank used in ground testing equipment for a domestically manufactured cryogenic upper stage (CUS). They came to the conclusion that the model's predictions closely matched the results of the experiments.

An "Experimental Investigation of Thermal Stratification in Cryogenic Tanks" was conducted by Minsuk Kang and Juwon Kim in (2017). In this study, the thermodynamic behaviour that takes place when cryogenic liquids, such as liquefied natural gas (LNG) and liquid hydrogen, are kept is examined. Using vacuum insulation with a thermal conductivity coefficient comparable to that of the polyurethane foam frequently used in LNG storage tanks, the experiment was carried out with liquid nitrogen and cryogenic liquid under 0.024 W/(m*K). Due to heat influx from the outside, cryogenic liquid contained in a tank typically exhibits various thermodynamic behaviours.

They came to the conclusion that, in particular, demonstrated the strong correlation between thermal stratification and thermal aspect ratio. Additionally, faster pressure rises are seen with the higher-level proportion, which is the opposite of what the homogeneous model would have anticipated. Even if much boil-off gas is produced in the early stages of a system with a high-level fraction, the rate at which it is produced is significantly lower than that indicated by the overall calculation in the homogeneous model. The study's findings demonstrate that the thermodynamic behaviours brought on by thermal stratification differ noticeably from those anticipated by the homogeneous model. As a result, these factors must be taken into account when designing and operating the connected equipment.

In their research, Abdullah Saleem and Shamsuzzaman Farooq (2018) An analysis of the boiling process and BOG production in a real-world LNG storage

tank using CFD simulation. An extensive dynamic CFD simulation of a regasification terminal's onshore full-scale LNG tank is shown. The axisymmetric VOF (Volume of Fluid) model is used to track the vapor-liquid interface, the Lee model is utilised to account for the phase transition, including the impact of static pressure, and LNG is approximated as pure methane. The boiling phenomenon is usefully illuminated by a thorough analysis of the heat ingress magnitude, internal flow dynamics, and convective heat transfer, which also yields a trustworthy estimate of the BOG. The dominating mechanism of boiling is surface evaporation, and with adequate insulation, nucleate boiling is improbable.

Their conclusion from the CFD simulation is that internal fluid circulation from natural convection causes the bulk liquid to become well mixed in around 20 hours. The vapour phase temperature, however, continues to be higher than the liquid phase temperature. This simulation work has demonstrated that small-scale experimental or numerical investigations cannot accurately represent the entire dynamic behaviour of a full-scale liquid storage tank when heat infiltration is present. The critical wall superheat that triggers nucleate boiling for LNG is determined to be independent of the tank sizes and pressures examined in this study, and it is in the range of 2.5 to 2.8 K.

To study the impact of slosh baffles on the pressurisation efficiency in a liquid hydrogen (LH2) tank, Zhan Liu and Cui Li (2017) developed a calibrated CFD model. When compared to the outcomes of the flying experiments, the calibrated CFD model is shown to have excellent predictive power. In-depth research has been done on the LH2 tank's pressure increase, thermal stratification, and wall heat transfer coefficient. According to the findings, slosh baffles significantly affect tank pressure rise, fluid temperature distribution, and wall heat transfer. Due to the presence of baffles, the stratification thickness steadily increases as tank axis and tank wall distances grow.

In contrast, in a tank without baffles, the stratification thickness first reduces and then increases as the distance from the axis increases. In a tank without baffles, a stratified thickness distribution of the "M" type is seen. It has been suggested to modify one heat transfer coefficient correlation with the fluid temperature change taken into account by multiplying a temperature correction factor. They discovered

that the average relative prediction errors of the heat transfer coefficient decreased for the dry tank wall from 8.93% to 4.27% and for the wet tank wall from 19.08% to 4.98%. Some of their insightful findings are Slosh baffles have a significant impact on the vapor-liquid interface's phase change, and the formation of thermal stratification is clearly influenced by the heat transfer from the vapour to the interface. These effects extend beyond the tank pressure increase, fluid temperature, and velocity distribution. In a tank with slosh baffles, where heat loads are focused below the baffles, the thicknesses of thermal stratification rise with distance from the axis. While the thermal stratification thicknesses in a tank without slosh baffles display a "M" type distribution below the interface, they initially reduce and subsequently grow with distance.

The development of a new analytical solution for the isobaric evaporation of a pure liquid cryogen by Felipe Huerta and Velisa Vesovic(2019). Expressions for the liquid volume, evaporation rate, Boil-off-Gas (BOG) rate, vapour temperature, and vapour to liquid heat transfer rate have been presented in particular. There have been both equilibrium and non-equilibrium scenarios taken into account. While in the latter, the vapour is viewed as being overheated in relation to the liquid and serves as an extra source of heat, the earlier model assumes that the vapour and liquid cryogen are in thermal equilibrium.

The numerical findings for the evaporation of liquid methane and liquid nitrogen in small, medium, and large storage tanks utilised in industry were compared to the derived solutions for two situations. The analytical answers are precise for the equilibrium model. With the exception of a brief transient period at the start of the evaporation, the analytical solutions for the non-equilibrium model are valid for the whole evaporation time. Regarding tangibles with industrial value. Their maximum variances are 1%, 2%, and 4.5%, respectively, and they provide precise estimations of liquid volume, BOG rate, and BOG temperature. The rate of heat transfer from vapour to liquid is likewise accurately predicted, with a maximum 5% variance. According to their findings, the equilibrium model's answers are precise independent of the tank's size or its cryogen content because the derivation only takes into account constant air temperature and continuous heat ingress via the tank's bottom. Except for a brief transient period at the start of the

evaporation, the analytical solutions for the non-equilibrium model are valid for the whole evaporation period.

They offer precise estimations of the three variables that are of great relevance to working engineers: liquid volume, BOG rate, and BOG temperature. The temporal evolution of the profiles is primarily controlled by the increase in the vapour height; the system reaches a pseudo steady-state with respect to heat ingress, and the increase in vapour temperature is a result of a lower volume of liquid being present. Although accuracy declines with storage tank size, the maximum deviations did not exceed 1% for liquid volumes, 2% for BOG rates, and 4.5% for BOG temperatures. They discovered that as tank diameter is reduced, the source term's contribution to the total heat infiltration increases. Therefore, compared to large storage tanks, the evolution of the vapour temperature profiles, which show enormous curvatures, is more influenced by heat entering from the outside than by conduction or advection. The numerical results and the analytical vapour to liquid heat transfer solution, Q_ VL, accord quite well. Even for the smallest tank, when Q_ VL contributes significantly and steadily grows, the greatest variation is less than 5%. This suggests that more intricate evaporation models can be constructed using the analytical answer for Q_ VL. The analytical solution's constant D will be tiny and the BOG rates will fall exponentially through evaporation, resulting in prolonged evaporation durations, if heat transfer through the bottom of the tank and heat transfer from vapour to liquid are less than heat transfer through the walls.

In order to store cryogenic flammables, Federica Ovidi and Elena Pagni (2019) carried out a numerical research of pressure buildup in vertical tanks. Large-scale cryogenic fluid storage facilities, like those for liquefied natural gas (LNG) and ethylene, are essential components of the chemical and petrochemical industries. Therefore, it is essential to model the thermal performance of such systems in order to improve the operations' safety and efficiency. The Volume-Of-Fluid technique and vaporization-condensation phenomena are applied in the current work to investigate the pressurisation behaviour of cryogenic storage tanks using computational fluid dynamics (CFD).

In order to solve the heat transfer through the tank insulation layers and eventually take into account accidental damages, the boundary conditions are

approximated from a 1-dimensional model. Prior to being expanded to include the simulation of an industrial cylindrical tank, the tank CFD model is first preliminary validated using small-scale experimental data collected for cryogenic nitrogen. Analysis is done on how fluid, such as ethylene and LNG (which is modelled as pure methane), fill level, and potential insulation damage affect natural convection, which drives liquid stratification and, eventually, tank pressurisation. They discovered that ethylene heats up and pressurises more quickly than methane. Due to a more effective natural convection flow, methane was shown to have a larger liquid thermal stratification than ethylene. The study could be a helpful tool for managing and making decisions regarding crucial processes, such as those involving cryogenic storage.

The completion of an experimental examination of the thermal behaviour in a cryogenic propellant tank under various pressurants by Kiyoshi Kinefuchi and Hideto Kawashima (2020). An important factor in the operation of cryogenic propulsion systems is the thermal behaviour of cryogenic propellant tanks. Here, ground tests were carried out in a liquid nitrogen-filled cryogenic tank with a 600 mm diameter. To examine its impact in relation to actual propulsion systems, gaseous helium and gaseous nitrogen (of the same species as the liquid) were utilised as pre-pressurants.

After pre-pressurization, the tank was shut so that the self-pressurization could be seen. Based on pressure and temperature readings, the tank's evaporation rate and heat flow were calculated. A thermal stratification model was also created after obtaining the axial liquid temperature distribution from the liquid draining from the tank bottom. They discovered that the temperature behaviour in the tank was greatly influenced by the kind of pre-pressurant. The helium pre-pressurization example showed a larger rate of evaporation, a higher rate of liquid internal energy rise, and a thicker thermal layer. The evaporation and development of the thermal layer were facilitated by the decreased nitrogen partial pressure in the helium example. Calculation of the tank's power balance revealed that the thermal layer and ullage were both heated by the tank's heat mass as well as by its ullage. Most of the evaporation happens where the tank skin and liquid surface first make contact. Under nitrogen pre-pressurization, the nitrogen vapour rises in a thin layer along the tank skin due to buoyancy; however, under helium pre-pressurization,

buoyancy is decreased, and a radial vapour flow is likely created from the contact point instead, resulting to a larger heat flux to the liquid.

The helium pre-pressurization example showed greater evaporation rate, higher liquid internal energy rise rate, and thicker thermal layer during the self-pressurization phase than the nitrogen case did. The evaporation and development of the thermal layer were facilitated by the decreased nitrogen partial pressure in the helium example. In the helium example, the power balance showed that the top flange's heat mass looked to be used for evaporation and an increase in internal energy. Evaporation mostly took place where the tank skin and liquid surface came into contact. Under nitrogen pre-pressurization, the nitrogen vapour rose in a thin layer along the tank skin due to buoyancy; however, under the helium mixture, the buoyancy was lower and a radial vapour flow could be produced from the contact point, resulting in a higher heat flux from the tank wall and ullage to the liquid. The helium and nitrogen pre pressurization examples showed different evaporation rates and thermal layer thicknesses, which suggests that the pressurant choice is important for cryogenic propulsion systems, particularly for multi-engine ignitions and long-duration in-space operation.

2.2 SUMMARY

- Researchers from all over the world have undertaken and published a wide range of experimental and numerical investigations on thermal stratification and self-pressurization of cryogenic storage tanks.
- However, a comprehensive investigation of stratification Study at elevated pressure and during vent off period is missing.
- The literature on stratification during venting off period is limited.
- The present project work aims to study the thermal stratification during vent off time in a cryogenic storage tank.

2.3 OBJECTIVES

- Develop an experimental setup to conduct the thermal stratification study.
- Conduct experimental studies on thermal stratification using liquid nitrogen in controlled condition.

- Conduct numerical study to validate the experimental result.

2.4 METHODOLOGY

- Literature review.
- Analysing the findings of the publications.
- Finding the research gap.
- Problem formulation.
- Develop a numerical model to predict the thermal stratification phenomena at elevated pressure during venting off period.
- Structural and thermal design of storage tank.
- Fabrication of the experimental set up.
- Modify the custom-made high-pressure tank with foam insulation.
- Experimental investigation using liquid Nitrogen.
- Compare the numerical model with the experimental result.

CHAPTER 3
COMPUTATIONAL FLUID DYNAMICS

3.1 INTRODUCTION TO CFD

Computational fluid dynamics (CFD) is a branch of fluid mechanics that uses numerical methods and algorithms to analyse and solve problems involving fluid flows. Computers perform the many calculations required to simulate how fluids and gases interact with the complex surfaces used in engineering.

3.2 APPLICATIONS OF CFD

- Hydrodynamics of ships
- Power plants, gas turbines, and IC engine combustion
- Wind loading; the external and internal environments of structures
- Lift and drag in aviation and vehicle aerodynamics

3.3 NUMERICAL METHODS USED IN CFD

Different methods used in CFD are

- Finite Element Method (FEM)
- Finite Difference Method (FDM)
- Finite Volume Method (FVM)

3.3.1 Finite Element Method (FEM)

The finite element approach divides the calculation domain into elements like triangular rectangles, tetrahedra, or rectangular parallelepipeds. These components are thought to be joined at specific joints called nodes. Here, a simple function can be used to calculate the field variable's fluctuation inside a finite element. These approximation functions are defined by the values of the field variables in each node. When field equations are built for the full continuum, the new unknowns are found at the nodal points. Resolving the field equations, which are commonly written as matrices, yields the node values of the field's variables.

3.3.2 Finite Difference Method (FDM)

The finite difference method is the most straightforward numerical technique used in the heat/diffusion equation's solution. The basic idea behind the method is to replace the numerous derivatives that result from the formal description of the problem with appropriate approximations on a finite difference mesh of nodes. The simplest derivation of finite difference formulas makes use of Taylor series. The final set of linear algebraic equations can be solved using any numerical technique.

3.3.3 Finite Volume Method (FVM)

The strategy that is most usually used is classic or conventional. The idea that the computation domain can be divided into various finite volumes is related to a different discretization method. Every finite volume is represented using this method as a line in 1D, an area in 2D, and a volume in 3D. The nodes of each finite volume act as the centre for computations. Rectangles are the most basic finite volumes in 2D rectangular Cartesian space. Each node's rectangle faces are made by drawing perpendiculars through the middles of its neighbouring nodes. To produce the discretization equations, the original partial differential equation is integrated across each finite volume. Using this method, nonlinear problems can be resolved with ease. Iterative methods are employed to get.

3.4 ADVANTAGES OF CFD OVER OTHER METHODS

- The amount of data points and tested configurations directly relates to the uneven cost of an experiment in terms of facility appoint or labour expenditures.
- The lead time and cost of a new design are significantly decreased as a result of CFD research.
- It offers essentially infinitely detailed results.

3.5 WORKING OF A CFD CODE

The three elements are

- Pre-Processor
- Solver
- Post-Processor

3.5.1 Pre-Processor

Technique of transferring a flow problem's input into a format that the solver can use using a user-friendly CFD application. During the pre-processing phase, user activities include, the geometry of the region of interest is defined by the computational domain.

- The geometry is defined by computational domain.
- Creating a mesh by dividing a large area into smaller.
- Deciding the physical and chemical events necessary for modelling.
- Specifying suitable border criteria for cells that are next to or in contact with the domain boundary.

The solution of a flow problem is found at the nodes inside each cell. The precision of a CFD solution is dependent on the number of cells in each grid.

3.5.2 Solver

- Using basic functions to approximate the unknown flow variables.
- Discretization through further mathematical procedures that involve substituting approximations into the governing flow equations.
- The resolution of algebraic problems.

3.5.3 Post-Processor

Similar to pre-processing, the post-processing field has recently seen a significant amount of development activity. many of which have great graphics capabilities. These consist of.

- Grid display and domain geometry
- Vectograms
- Contour plots with lines and shade
- Surface plots in 2D ,3D
- Element monitoring
- Output in colour
- View adjustment

These plots and contours help us to visualize the problems to a great extent and a thorough understanding of the situation can be attained.

CHAPTER 4

EXPERIMENTAL INVESTIGATION

The evolution of stratification inside a cryogenic storage tank can be completely understood by conducting ground experiments. For this, a specially created high-pressure cryogenic storage tank is designed and constructed as part of an experimental setup. The safety of the vessel has been ensured by structural and thermal design under all operational circumstances. The construction material is stainless steel 304, and foam insulation is offered to lessen heat transfer. The cryogen employed is liquid nitrogen. Six PT 100 temperature sensors were put in the tank's inner vessel and spaced apart vertically by 43.5 mm each to conduct the stratification investigation.

Figure 4.1 shows the experimental set up used for this study. It consists of a test Dewar and accessories, ladder temperature sensor arrangement, cryogen storage tank, data acquisition system etc. A pressure gauge is used to monitor the pressure inside the tank continuously.

Fig 4.1: Experimental Setup

4.1 COMPONENTS OF EXPERIMENTAL SET UP

4.1.1 Custom-Made High-Pressure Test Tank

The 2.2-liter test tank utilised in this investigation has a design pressure of 4 bar absolute and can store liquid nitrogen. A stainless steel 304 vessel serves as the test tank. The tank has a flat finish at the bottom and measures 103mm in outer diameter and 281mm in height. The vessel has a 1.5mm thickness. To lessen heat transfer from the surrounding environment, 23mm thick foam insulation is provided at the bottom and around the circumference. The vessel is constructed of stainless steel, which is more durable. Due to its extremely low thermal conductivity, conduction heat transmission is minimised. The test tank employed in this investigation contains welded joints, and the top of the tank provides access to the interior. Six PT100 temperature sensors with an accuracy of less than 0.2% are mounted vertically on a short stainless-steel tube inside the inner shell. The temperature sensor T6 is placed 10mm from the tank bottom and is kept at a distance of 43.5mm from the other sensors. The tests are carried out in an ullage space of 0.2 litres.

Two instruments are mounted on the tank's top: a mechanical pressure gauge with an accuracy of 0.5% and a relief valve. The neck region of the vessel is the only thermal interface with the environment, and during the experiment, water vapour generation is apparent.

Fig 4.2: Custom made Test Tank

4.1.2 Relief Valve

The relief valve is a kind of safety valve used to limit the pressure developed inside the cryogen storage container. The design pressure of the relief valve is 4 bar, which means the valve gets actuated when the operating pressure inside the container reaches beyond 4 bar. It allows the gases to flow through it until the pressure inside the vessel comes to its reset value. Figure 4.3 Shows the pressure relief valve.

Fig 4.3: Pressure relief valve

4.1.3 Temperature Sensors

PT100 sensors are used to measure the temperature at different levels of the vessel, which is kept at a distance of 43.5mm with accuracy of ±0.2 %. The sensors are mounted vertically on a narrow stainless-steel tube. Figure 4.4 Shows the thermocouple which is used for the temperature measurement.

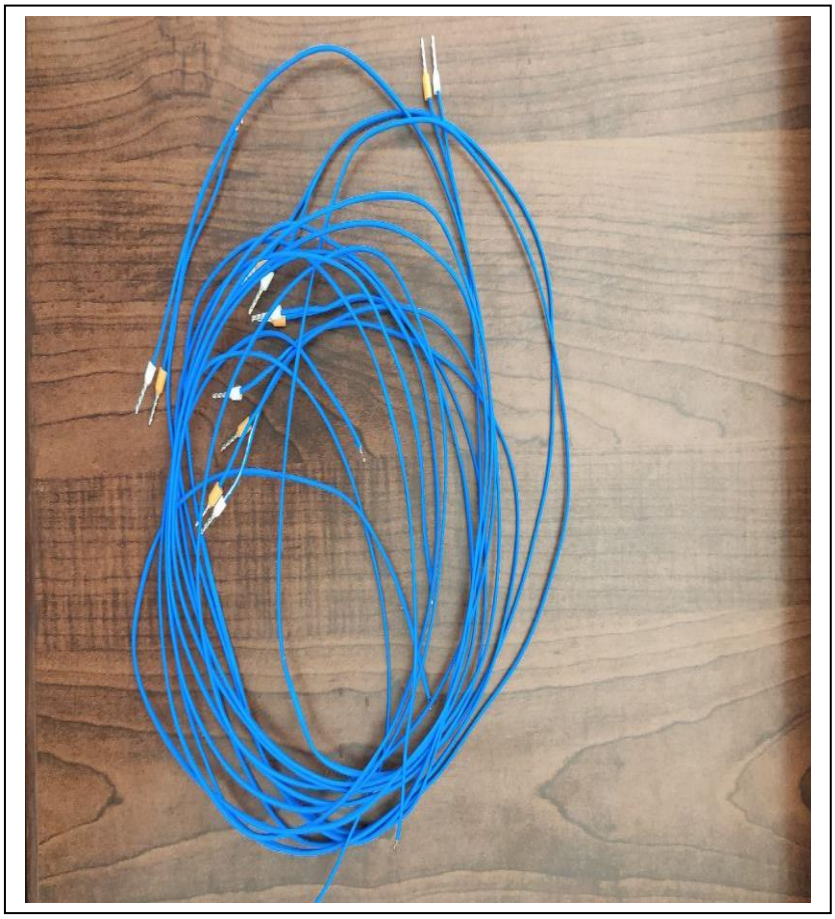

Fig 4.4: Thermocouple

CALIBRATION OF THERMOCOUPLE

The setup for calibrating the thermocouples used in the experiment is shown schematically in Fig. 4.5. T-type thermocouples are used in the currently being conducted experimental work. The thermocouple bulbs are produced via gas welding. The bath oil, which is kept at a constant temperature, is submerged with the thermocouple bulb. The other end of the thermocouple is connected to a temperature 31 scanner. The temperature of the bath is kept constant, and a temperature scanner records the temperature as it is measured.

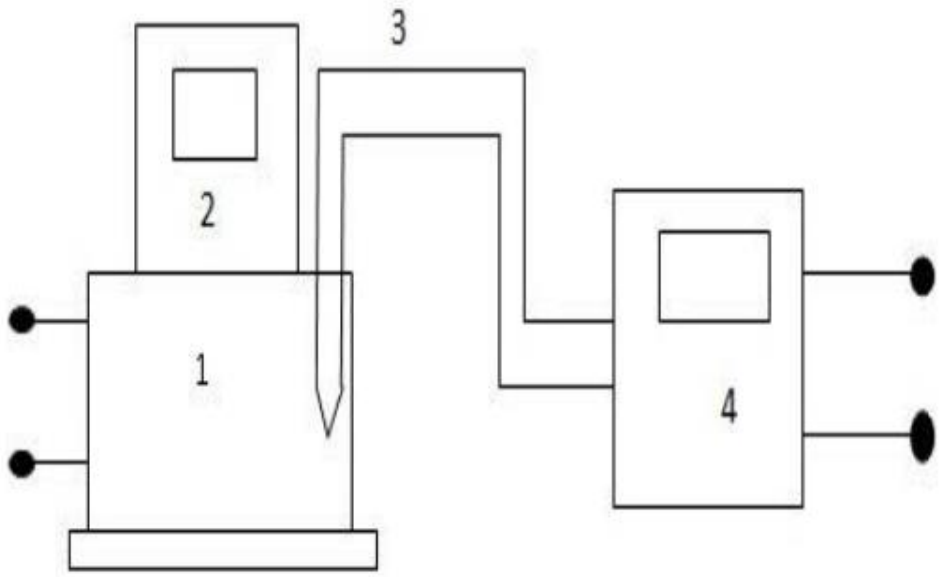

1. Constant temperature bath 2. Temperature display 3. Thermocouple
4. Temperature scanner

Fig 4.5: Schematic layout of Thermocouple calibration

Table 4.1 Calibration data for thermo-couple (TC-01)

Sl.No	Set Temperature(C)	Observed Temperature(C)	Error
1	25	25.05	0.05
2	35	35.66	0.66
3	45	45.14	0.14
4	55	54.87	-0.87
5	65	64.82	-82

Table 4.2 Calibration data for thermo-couple (TC-02)

Sl.No	Set Temperature(C)	Observed Temperature(C)	Error
1	25	25.02	0.02
2	35	35.64	0.64
3	45	45.13	0.13
4	55	54.87	-0.87
5	65	64.8	-0.8

Table 4.3 Calibration data for thermo-couple (TC-03)

Sl.No	Set Temperature(C)	Observed Temperature(C)	Error
1	25	25.05	0.05
2	35	35.60	0.60
3	45	44.11	-0.11
4	55	54.90	-0.90
5	65	64.75	-0.75

Table 4.4 Calibration data for thermo-couple (TC-04)

Sl.No	Set Temperature(C)	Observed Temperature(C)	Error
1	25	25.03	0.03
2	35	35.61	0.61
3	45	45.14	0.14
4	55	54.84	-0.84
5	65	64.75	-0.75

Table 4.5 Calibration data for thermo-couple (TC-05)

Sl.No	Set Temperature(C)	Observed Temperature(C)	Error
1	25	25.06	0.06
2	35	35.59	0.59
3	45	45.16	0.16
4	55	54.9	-0.09
5	65	64.77	-0.77

Table 4.6 Calibration data for thermo-couple (TC-06)

Sl.No	Set Temperature(C)	Observed Temperature(C)	Error
1	25	25.01	0.01
2	35	35.67	0.67
3	45	45.14	0.14
4	55	54.91	-0.91
5	65	64.81	-0.81

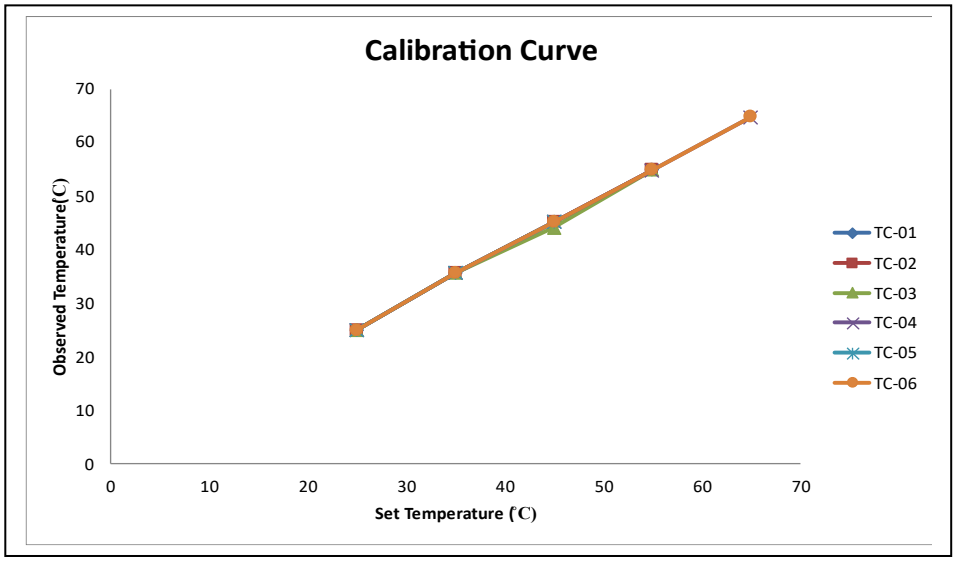

Fig.4.6 Thermocouple Calibration Curve

55

4.1.4 Pressure Gauge

A mechanical pressure gauge with accuracy of ± 0.5 % is mounted at the top of the vessel to measure the pressure of the storage tank. It is welded to the stainless-steel plate which is leak proof tested.

Fig 4.7: Pressure gauge

4.1.5 Data Acquisition System

continuous measurement of temperature was made possible by a data acquisition system. Data acquisition is the process of measuring a physical phenomenon with the help of a computer. Readings were recorded at a time interval of 5 seconds.

Fig 4.8: Data Acquisition System

4.2 DESIGN OF CUSTOM-MADE TEST VESSEL

The design procedure of a cryogenic vessel consists of structural and thermal design.

1. Structural design:

There are a number of safety risks associated with storing cryogen in a cryogenic vessel, but they are all intended to lower the risk that comes with it. First of all, no Dewar can offer the ideal insulation, and as the cryogenic liquid slowly boils away, a large amount of gas is produced. For instance, nitrogen expands 1 to 696 times from its boiling point to the ambient temperature. As a result, the sealed Dewar can develop under very high pressure, and safety measures are necessary to reduce the likelihood of an explosion. In general, an ASME code section VIII, Division I cryogenic Dewar vessel (Pressure vessel) specifies an internal pressure range of 0.1 MPa to 30 MPa.

2. Thermal design:

Thermal design is conducted on the system to measure the various heat inleaks, the evaporation rate of the vessel is measured from the thermal load calculation and is obtained as 3.22 l/day.

4.2.1 Structural Design

There are a number of safety risks involved with storing cryogen in a cryogenic tank, however they are all intended to lower the danger that comes with it. First of all, no Dewar can offer the ideal insulation, and as the cryogenic liquid slowly boils away, a large amount of gas is produced. In general, an ASME code section VIII, Division I cryogenic Dewar vessel (Pressure vessel) specifies an internal pressure range of 0.1 MPa to 30 MPa.

Product container

- Explosion of the product container due to internal pressure.
- Hoop and longitudinal stress developed on the surface of the product container.

Flange

- Minimum thickness of the flange.
- Hydro static end force.

Assumptions

- The material used for fabrication (SS304) is considered as perfect alloy without metal defect.
- Weld efficiency of all welded joints are taken as 100%.

Specifications:

Pipe used: 4" SCH 10S
Outer diameter: 114.3 mm
Inner diameter: 108.2 mm
Length of pipe: 1400 mm
Radius of vessel, r = 57.15 mm
Thickness t = 3.05 mm
For thin shell assumption, the radius to thickness ratio should be greater than 10.

$$\frac{\mathrm{R}}{\mathrm{t}} = \frac{57.15}{3.05} = 18 \qquad \frac{r}{t} > 10, \text{thin shell assumption can be considered.}$$

Stresses acting:

For a cylindrical vessel under an internal pressure condition, the hoop stress and longitudinal stresses are developed along the surface,
we have,
P = Working pressure=0.4 MPa.
R = radius = 0.054 m
t = Shell thickness = 0.003 m

$$PL \times 2R = 2 \times \sigma hoop. \mathrm{T}$$
$$P \times R = \sigma hoop \times t$$

$$\sigma hoop = 0.4 \times \frac{0.054}{0.003}$$

$$\sigma hoop = 7.2\text{Mpa}$$

To determine the longitudinal stress, consider a cross section of the product container perpendicular to its axis.

$P \times \pi R\ 2 = \sigma_{long} \times (2\pi Rt)$

$\sigma_{long} = 0.4 \times 0.054/2 \times 0.003$

$\sigma_{long} = PR/2t$

$\sigma_{long} = 3.6\text{Mpa}$

The yield strength of SS 304 at 77 K is 1300 MPa. The hoop and longitudinal stress developed on the surface of the vessel is much below the yield strength of the material.

Design of flange

Hydrostatic end force on area inside of the flange, H_D

$H_D = \frac{\pi B^2 P}{4}$

$H_D = \pi \times 0.100^2 \times 4 \times \frac{10^5}{4}$

$H_D = 3141.59\ \text{N}$

So, the pressure forces on the flange = 3141.59 N

Gasket load under operating condition = 347910.0236 N

Moment due to hydrostatic force, MHD

M_{HD} = $H_D h_D$

$hD \times 2 = Cb - B$

h_D=0.001

M_{HD} = 3141.59 × 0.001

M_{HD}=3.14159 Nm

Moment due to gasket load, MG

M_G = $H_G h_g$

$h_G \times 2 = C_b - G$

$h_G = 6 \times 10^{-3}$

$M_G = 347910.02 \times 6 \times 10^{-3}$

M_G =2087.46 Nm

Total moment = 4237.75 Nm

flange thickness, t_f

$$t_f = \sqrt{\frac{m_f y}{f_t B}}$$

y is the hub factor, $\frac{A}{B} = \frac{22.9}{10.8} = 2.12$

y = 2.74

$$t_f = \sqrt{\frac{423775 \times 214}{515 \times 10^6 \cdot 0.10}}$$

t_f =0.0150m

Minimum required 0.0150 m

Flange used = 0.03m, so design is safe.

4.2.2 Thermal Design

Thermal design is conducted on the system to measure the various heat inleaks, and significant possibilities are:

- Heat load by conduction
- Heat load by conduction
- Heat transfer through radiation

Material used = SS304

SS 304 is ideal for the fabrication of experimental test tanks.

Heat transfer through the sensor line

Q_1 =0.1946 W

Heat transfer through the fill line

Q_2 =0.1946 W

Heat transfer through the insulation

$Q_3 = -\frac{KAdt}{dx}$

$Q_3 = -2 \times \pi \times 0.057 \times 0.3 \times \frac{223}{0.03} = 0.798$ W

Total heat transfer ratio into the vessel

$Q = Q_1+Q_2+Q_3$

$Q = 0.1946+0.1946+0.798 = 1.1872$ W

Determination of evaporation rate

Maximum heat load possible = 1.1872 W

Latent Heat of Evaporation = 200 J/g

Evaporation rate = $\frac{1.1872}{200} = 5.936\times10^{-3}\ \frac{g}{s}$

Density of LN_2 at 77 K = 790

Evaporation rate of liquid Nitrogen = 5.14 l/day

convective heat transfer coefficient,

$$h_c = \frac{1}{2}\left[\left(\frac{K_f^3 \rho_f^2 g \Delta T}{\mu_f^2 T_f}\right)\right]^{0.25} \left[\frac{\Delta T}{L}\right]^{(}$$

T1 = 80K

T2 = 300K

K_f = 1.8 × 10^{-4} W/cm.K

ρ_f = 1.8 × 10^{-3} g/s

μ_f = 120 × 10^{-6} Poise

C_p = 1.04 J/g.K

g= 980 cm/s^2

h_c =1.028×10^{-3} W/cm^2K

Total heat transfer,

Q = h_cAdT

Q= 1152.40 W

4.3 EXPERIMENTAL SET UP

Based on the design procedures and other requirements, an experimental set up is fabricated and installed. Figure 4.9 shows the detailed instrumentation provided at the top of the tank.

Fig 4.9: Experimental Set Up

4.4 EXPERIMENT PROCEDURE

The experimental set up was completely installed and ensured all the components used for the experiment were in operating condition. Initially the temperature sensors are connected to the data acquisition system and runs for a test to ensure that all the sensors show the ambient temperature. Figure 4.10 shows the connection of sensors to the data acquisition system.

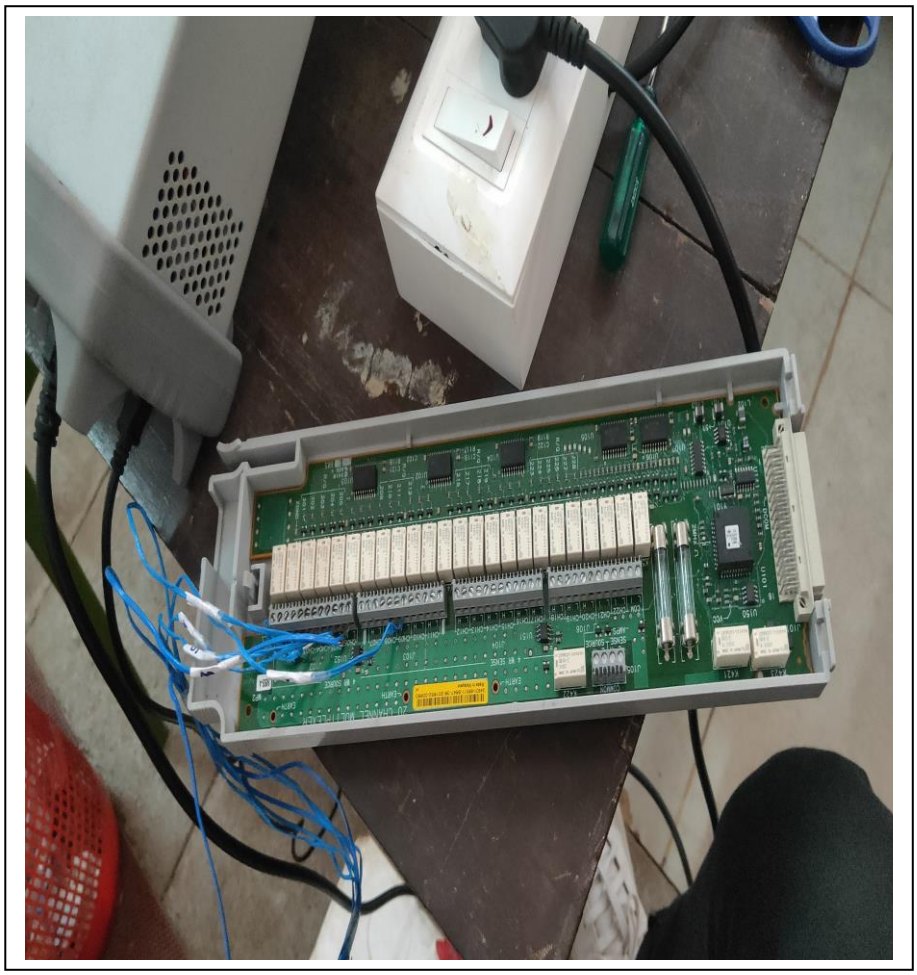

Fig 4.10: Connection of Sensors to the Data Acquisition System

Once the sensors show the ambient conditions, it is ready to pour the liquid nitrogen to the test tank. During liquid pouring, a huge amount of gaseous nitrogen is evolved and escaped to the atmosphere. So, during liquid nitrogen pouring time lot of liquid will be lost due to the chilling process. Figure 4.11 shows the filling of the liquid nitrogen to the test tank.

Fig 4.11: Filling of the Test Tank

After filling the test tank to a volume of 2 litres, the top flange is bolted tightly to reduce the heat inleak. Figure 4.12 represent the completely filled test tank.

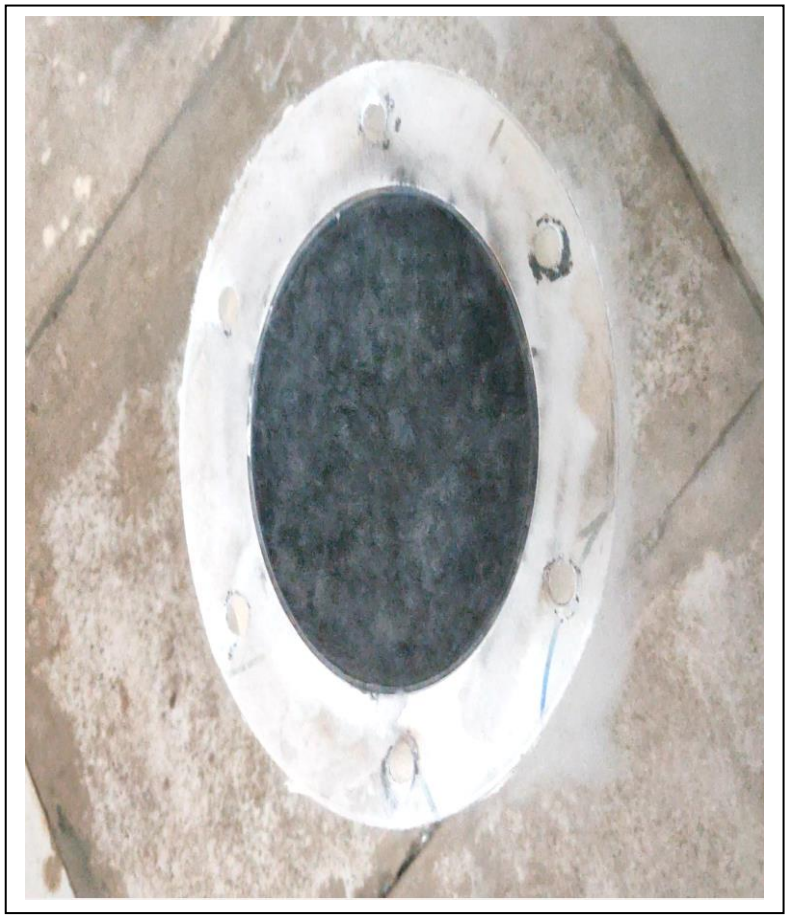

Fig 4.12: Completely filled Test Tank

During the closing time of the top flange, the vent valve should be kept open to reduce risk of pressure build up, the sensors are connected to the top flange, so during the closing time of the top flange the sensors will be come in contact with the liquid nitrogen and the sensors will start to show the negative temperature. Figure 4.13 shows the completely closed vessel.

Fig 4.13: Completely closed Vessel

Once the required fil level is maintained, the vent valve is closed, and we can see the pressure starts building. All the temperature sensor readings were recorded at an interval of 5 seconds using a data acquisition system. Figure 4.14 shows the pressure building process.

Fig 4.14: Pressure building process

Once the pressure is reached to the maximum value of 4.71 Bar, the vent valve is opened suddenly and the temperature changes are recorded. It takes about 4176 Seconds to reach this pressure. Figure 4.15 represents the venting process.

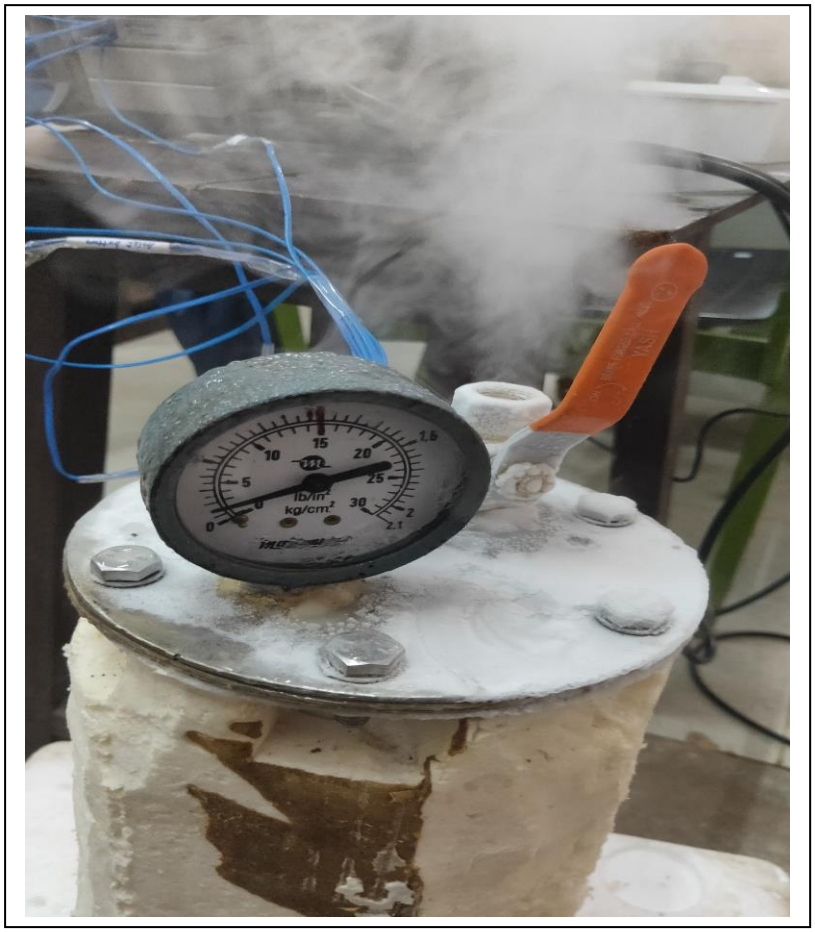

Fig 4.15: Venting process

4.5 DETAILS OF CRYOGENIC STORAGE VESSEL

Product container:

Material: 4” SCH 10 S Pipe

Outer diameter = 114.3 mm

Inner diameter = 108.2 mm

Length = 281 mm

Thickness = 1.5 mm

Flanges:

Outer diameter = 126 mm

Thickness = 4 mm

Insulation used:

Foam insulation

4.6 SUMMARY

A custom-made test tank is designed to study thermal stratification phenomena inside a cryogenic storage tank during venting period. The design includes the thermal and structural to ensure that it can be work at the high pressure safely. Liquid nitrogen is used as the cryogen. A test tank of 2.2 litres used in this experiment and it can withstand 4 bar pressure. Stratification during venting at elevated pressure is tested.

CHAPTER 5

NUMERICAL SIMULATION

This chapter discusses the creation of a CFD model to investigate the stratification phenomenon. Numerical models can be used to conduct extensive studies with less time, money, manpower, and equipment. The simulation is done using the commercial Ansys Fluent programme.

5.1 DEVELOPMENT OF NUMERICAL MODEL

To comprehend the fluidic and thermodynamic phenomena during the self-pressurization period, a multiphase 2D axis-symmetric cylindrical tank partially filled with liquid nitrogen is used. Both liquid and vapour nitrogen were present at their saturation conditions, which correspond to atmospheric pressure (101.3 kPa). The simulation employs a time-dependent VOF (Volume of Fluid) approach. The volume fraction of two phases added together in each control volume equals one.

5.1.1 Approaches to Multiphase Modelling

The multiphase numerical calculation is based on two methods:

a. The Eulerian – Lagrangian approach:

fluid phase is treated as a continuum by solving the time-averaged Navier-Stokes equations. The dispersed phase (which constitutes a large number of particles, bubbles or droplets) is solved by tracking them throughout the flow field of interest. The dispersed phase can exchange momentum, mass, and energy with the fluid phase. This model is suited for cases where the dispersed phase has a very low volume fraction; it is inappropriate for modelling liquid-liquid mixtures.

b. The Eulerian – Eulerian approach:

Solves the dispersed phase as an ensemble of individual discrete phases flowing like another fluid in the flow system. Since any control volume is occupied by both phases, the fraction of phasic volume is used. These volume fractions are assumed to be continuous functions of space and time, their sum being equal to one. Conservation equations are computed for each phase to achieve a set of equations.

5.1.2 Volume of Fluid Method

To determine the variation of the interface, the VOF method is adopted in which the changes happening at the interface of each cell are located by solving the continuity equation for the volume fraction of the second phase.

5.1.3 Boundary Conditions and Assumptions

Assumptions:

1. Heat transfer from ambient is considered as steady.
2. The tank pressure is assumed to be uniform throughout the ullage.
3. The heat transfer across the liquid-vapor interface is due to natural convection and steady.
4. The liquid-vapor interface temperature represents the saturation value corresponds to the pressure of the cryogenic tank.

Boundary conditions:

1. At the bottom and top surfaces, the walls are adiabatic.
2. On the side walls,

$$-K\frac{\partial T}{\partial n} = q_w$$

5.1.4 Numerical Implementation

- A two-dimensional cylindrical tank of 0.2 m height and 0.099 m inner diameter is used for the simulation.
- The CFD package Ansys 19.2 is used for this work.
- A constant heat flux of 10 W/m2 is applied on the sidewall.
- The pressure-velocity coupling algorithm selected is SIMPLEC (Semi-Implicit Method for Pressure-Linked EquationConsistent). The converged

solution is easy to achieve by using this method rather than a SIMPLE algorithm.

- Since the problem is transient, a time step of 0.001 s is selected so that the Courant number is less than 0.1.

Figure 5.1 shows the mesh details of the geometry,

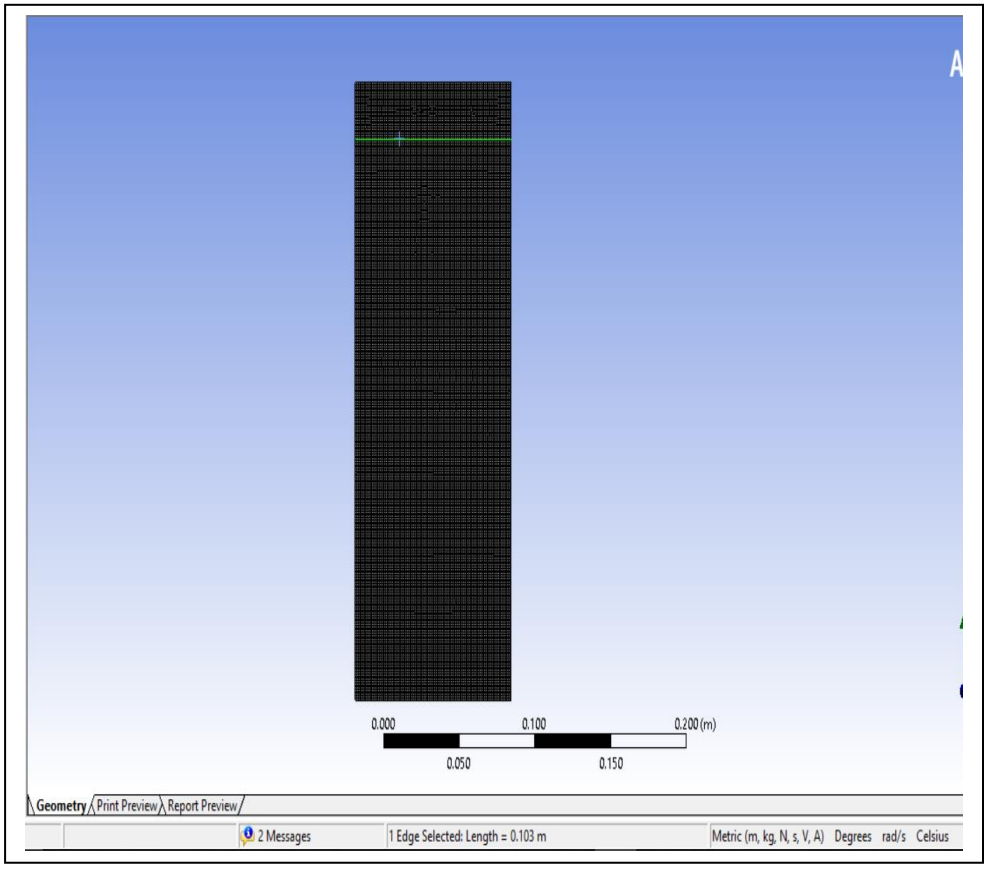

Fig 5.1: Mesh details

5.1.5 Grid Independency Study

six grid system with element size of 0.001,0.0009,0.002,0.0007,0.0008 and 0.003 are used. Table 5.1 shows the details of the grid independent study. It shows the variation of average temperature inside tank with mesh number. The average temperature for two grids (35673 and 45277) is same. The grid with 28938 mesh

number are shows almost accurate temperature. Figure 5.2 shows the graph of the grid independency study.

Table 5.1 grid independent study

	Model no:1	Model no: 2	Model no: 3	Model no: 4	Model no:5	Model no:6
Element size	0.003	0.002	0.001	0.0009	0.0008	0.0007
Number of elements	3203	7332	28938	35673	45277	59094
Average temperature(K)	80.27	77.858	77.807	77.836	77.836	77.834

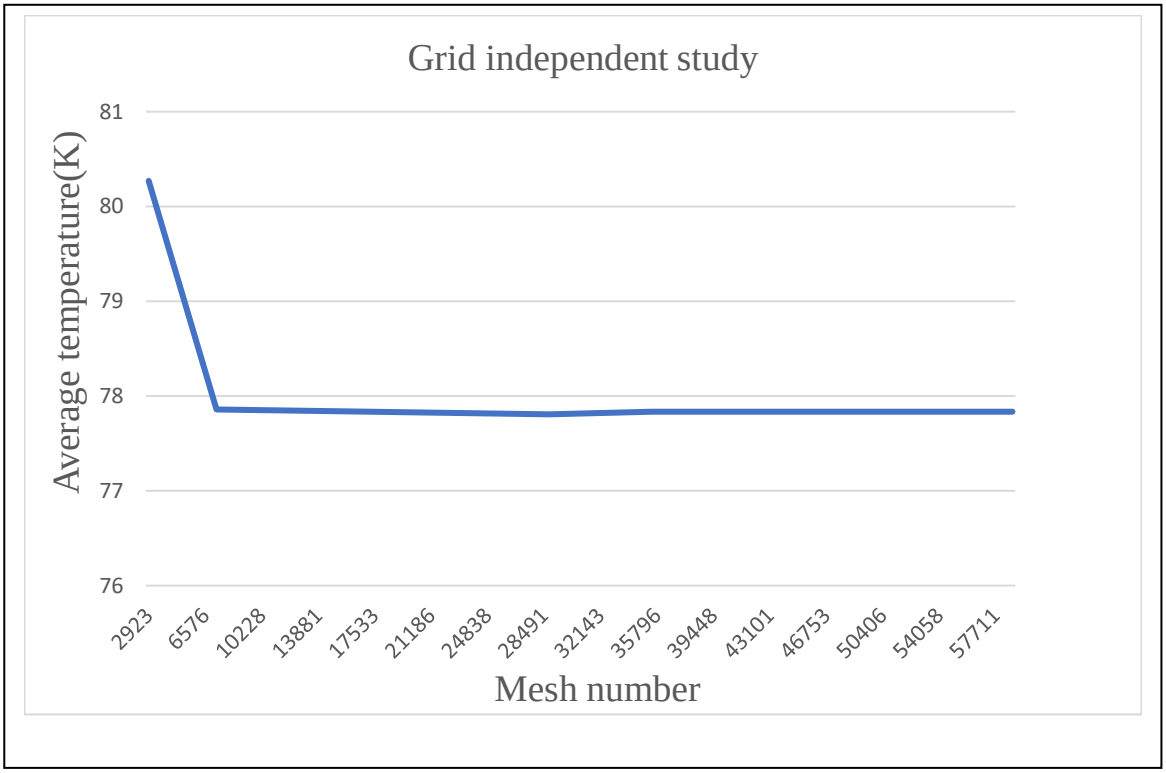

Fig 5.2: Grid Independency Study

5.2 MODEL VALIDATION

5.2.1 Validation with Experiments Conducted

Validation of the numerical model is required to consider the self-pressurization of the cryogenic tank. The experimental findings from the PG lab are used to validate the numerical model's output. A cylindrical tank with a diameter of 0.1 m and a height of 0.281 m makes up the experimental setup. Liquid nitrogen was employed as the cryogen. On the sidewall, 10 W/m^2 continuous heat flux was applied. Insulated bottom. The initial pressure and temperature of the liquid and vapour were 1.0980 Pa and the saturation point, respectively. A 50-second period of self-pressurization was recorded, and the results were compared with numbers. The comparison of the experimental and numerical results is shown in Figure 5.3. Figure 5.3 shows the comparison of the experimental and numerical results. The pressure and temperature obtained from the experimental investigation is greater than the result obtained from the numerical result.

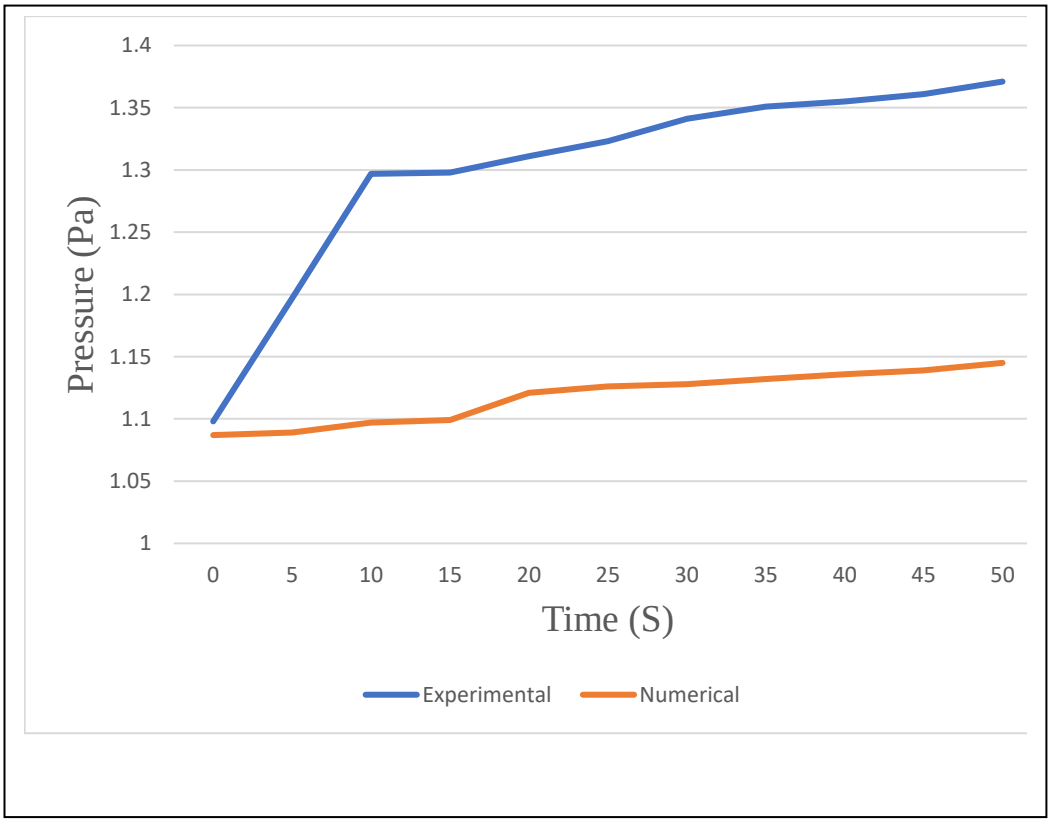

Fig 5.3: Validation of the numerical model with experimental result

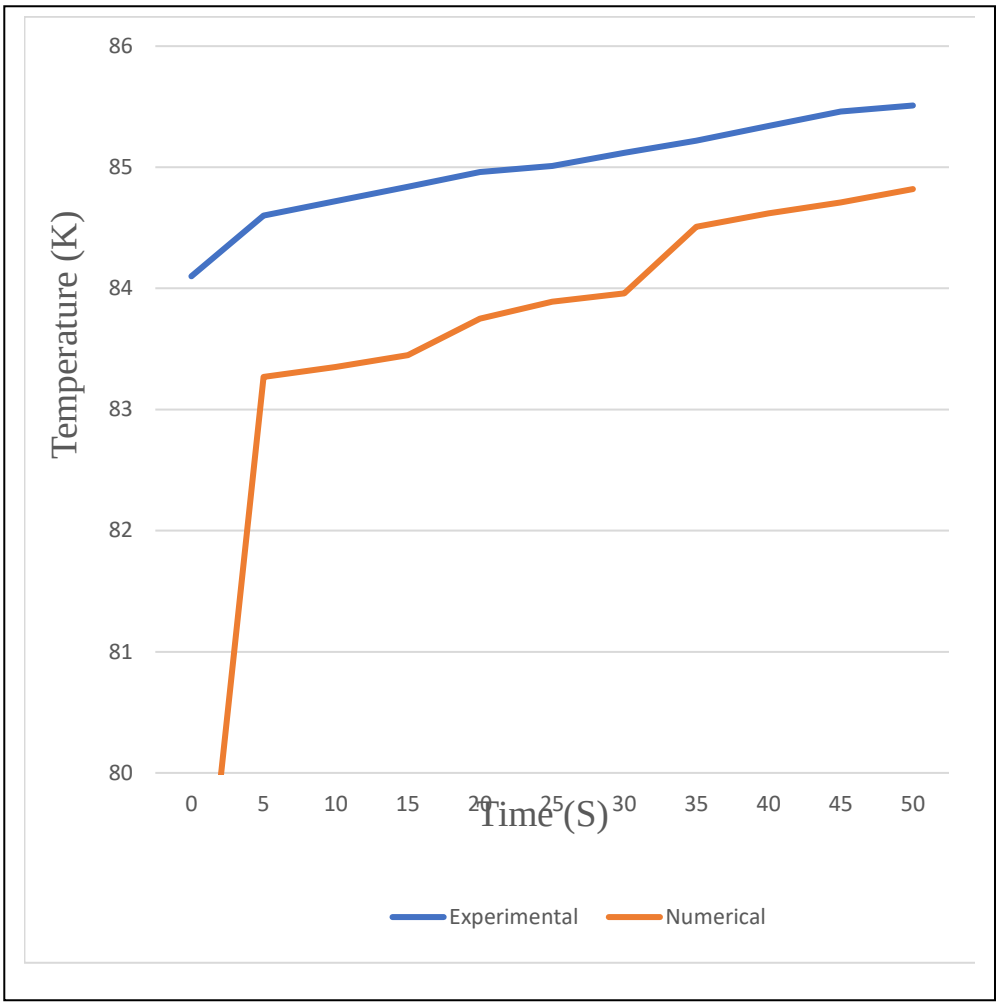

Fig 5.4: Validation of the numerical model with experimental result

5.3 SUMMARY

To comprehend the thermodynamic and fluidic phenomena occurring inside a propellant tank partially filled with liquid nitrogen, a numerical model was created. The movement of the liquid-vapor boundary is predicted using the Volume of Fluid (VOF) approach. The findings were confirmed by experimental findings from TKM Engineering College Kollam's PG lab. This model provides a clear understanding of the production of the stratified layer, fluid velocity, and heat transmission processes.

CHAPTER 6

RESULTS AND DISCUSSION

This chapter includes the observations, inquiries, and critical discussions from the analytical, experimental, and numerical works performed on the cryogenic storage vessels for the in-depth study of thermal stratification and self-pressurization. These activities allow for the formulation of reasoned conclusions and act as the basis for determining the scope for further research.

6.1 ANALYTICAL MODEL FOR THE PREDICTION OF STRATIFICATION

6.1.1 Prediction of Stratification Parameters

The Ansys 19.2 has been used to create an analytical model. The thermal stratification in a cylindrical liquid nitrogen tank with a 0.103 m diameter and 0.28 m height has been explored using the proposed model. A 50-second time frame is used for stratified layer prediction. The time frame was chosen so that by the end of it, the stratified layer would have fully grown throughout the tank.

6.2 EXPERIMENTAL INVESTIGATION OF THERMAL STRATIFICATION

To completely comprehend the thermal stratification phenomenon and the evolution of pressure in a cryogenic storage tank, experimentation is required. A 2.2 L capacity cryogenic storage tank is created for the experimental research. The critical findings are covered below.

6.2.1 Stratification During Venting

The cryogenic storage tank is made up of SS 304 with foam insulation. During the pouring of liquid nitrogen, the initial chilling of the tank happens and the inside temperature drops to liquid nitrogen temperature. The process of initial chilling is depicted in Figure 6.1.

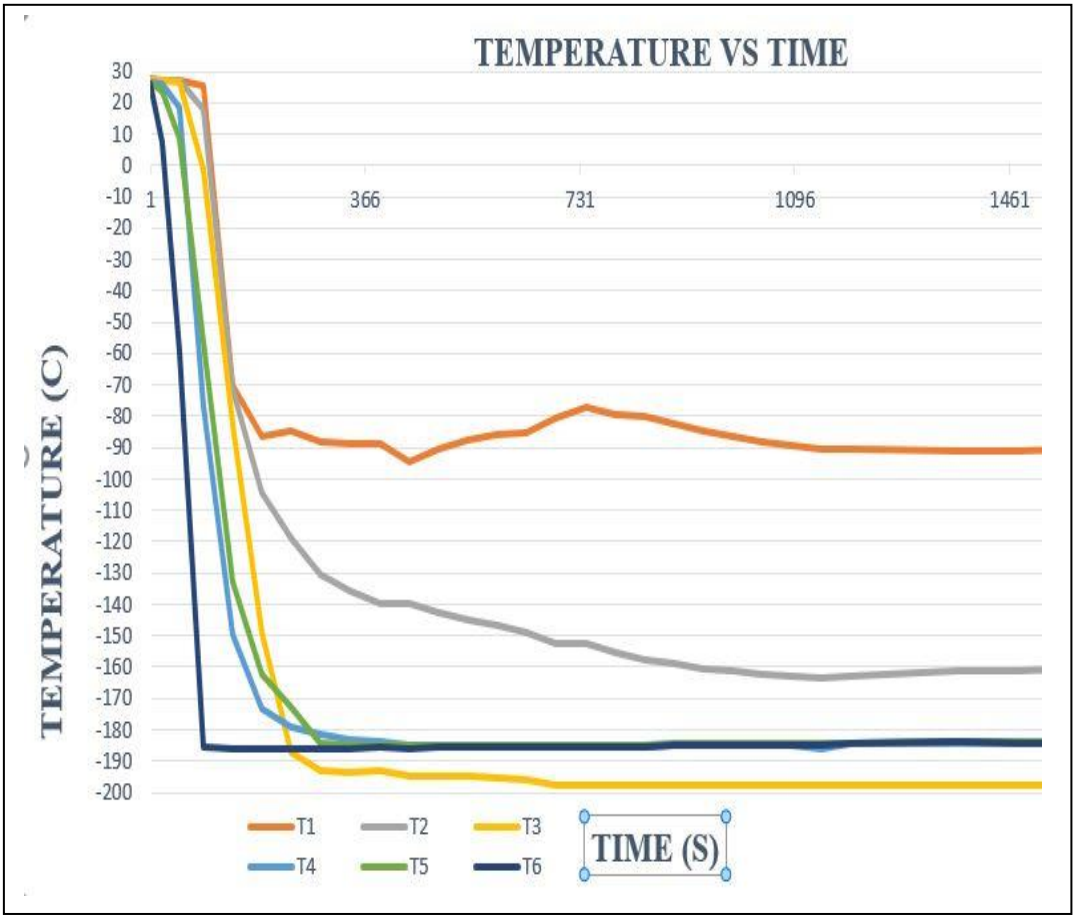

Fig 6.1: Initial chilling

Figure 6.1 shows that the sensors measure the temperature of liquid nitrogen from T2 to T6. The maximum ullage temperature value is around 224 K initially, which is at the top of the tank T1. Once the liquid is filled to the desired level, the top lid of the tank is bolted and the vent valve will keep open to remove the vapour generated inside the ullage space due to chilling process. After the chilling process the sensors will shows the liquid nitrogen temperature, at that time the vent valve is closed for the pressure build up process. Temperature and pressure inside the tank are continuously monitored to study the evolution of pressure and stratification

inside the cryogenic storage tank. Stratification during venting and non-venting conditions were studied.

During venting, the vessel is exposed to the atmosphere. Hence, the saturation temperature of the liquid remains close to the normal boiling point. No significant thermal stratification is visible.

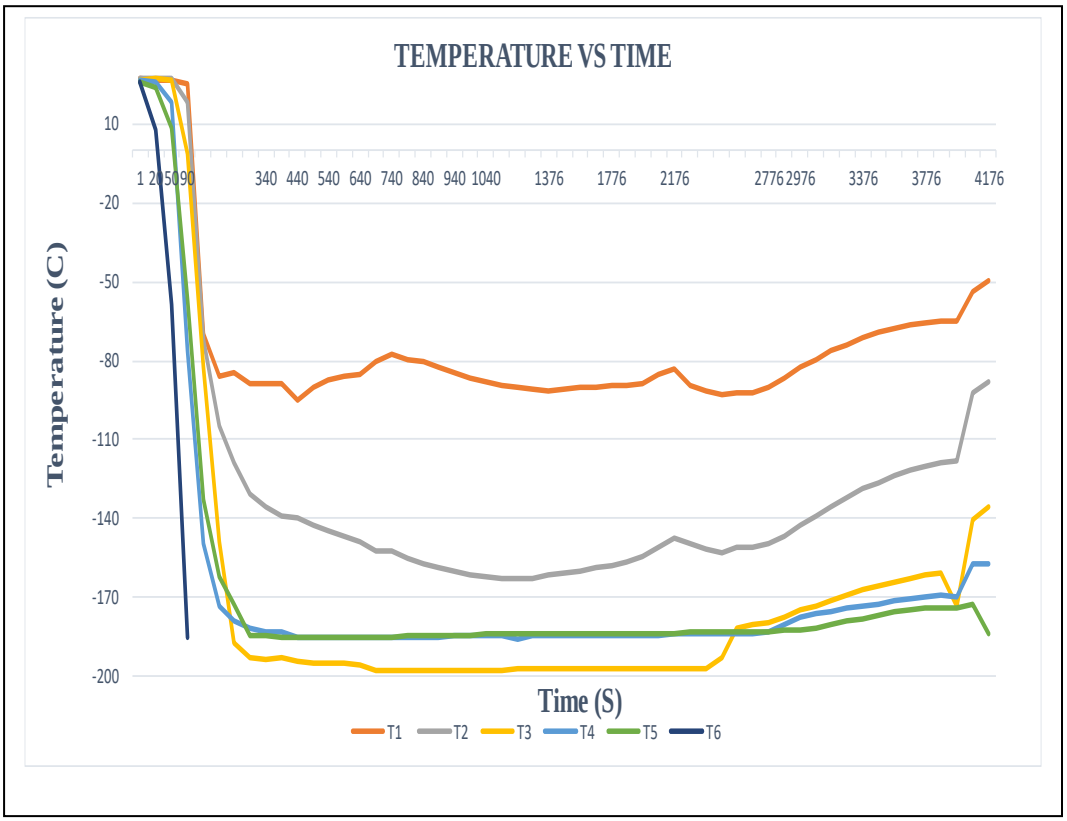

Fig 6.2: Temperature Vs Time graph

Without venting, the height of the tank and a sizable temperature difference are both present. The interface between the tank bottom and bottom has a maximum temperature difference of 7 K. The rate of temperature increase across the tank's various regions appears to fluctuate. In comparison to the bottom temperature, the slope of the curve corresponding to interface temperature is larger. This is as a result of the buoyancy force's induction of an upward convection stream. Furthermore, there is considerably less heat transfer between the stratified layers thanks to liquid nitrogen's low thermal conductivity. Temperature rises over time as warmer liquid at the contact accumulates more and more.

The Figure 6.3 shows the evolution of pressure inside the tank. During the interval of 24-51 minutes, a significant pressure rise is discernible. There will be a significant amount of evaporation at the liquid-vapour interface during the initial transient pressurisation interval. The liquid close to the wall rises during this time due to buoyancy and arrives at the liquid-vapour contact. It bends downward to the bottom after arriving at the interface, turning to face the axis. However, due to viscosity and buoyancy forces, the fluid begins to lose momentum as it descends and turns once more towards the wall. The liquid is well mixed in the horizontal plane as a result of this radial movement, and the temperature difference will be small and highly localised. With increasing time, a steady stratified flow field forms and after that, no noticeable change happens. Also, the presence of vortex-like and well-mixed flow below the interface causes localized temperature changes. These may be the reason behind the temperature changes during the initial transient pressurization period.

Heat transfer through the top side is high and also the aspect ratio of the tank is very high, which may increase the rate of self-pressurization. This will cause the self-pressurisation and temperature increase.

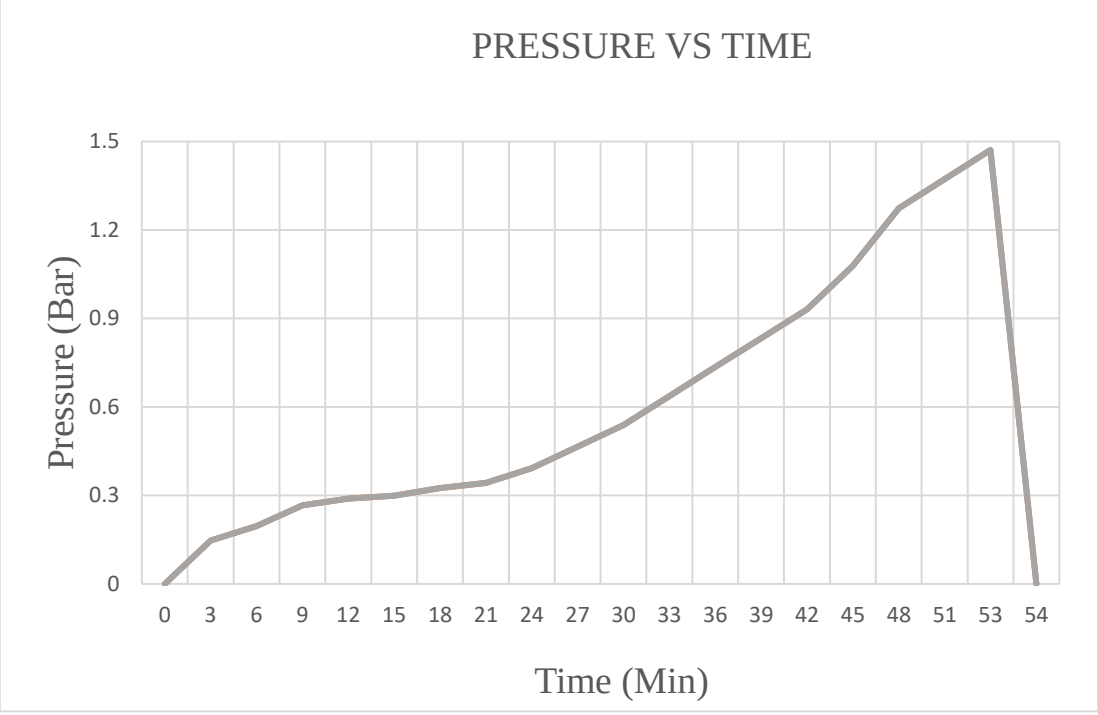

Fig 6.3: Pressure Vs Time graph

6.3 RESULTS OF NUMERICAL SIMULATION

Ansys Fluent is used to build a numerical model to better understand the thermodynamics of self-pressurization and thermal stratification. The results of the experiments support the model's validity. The following lists the various judgments made by numerical analysis.

6.3.1 Study of Stratification in a LN2 Tank

A numerical study has been conducted on a cryogenic storage tank that holds LN2. The tank's geometry is identical to that of the trials; non-venting situations are modelled. After the initial operations of chilling and level correction, the vent valve in the non-venting experiment closed. The initial liquid temperature is 79.1 K and there is no gradient in the starting liquid temperature. At the liquid-vapor interface, there will be a significant quantity of evaporation during the first transient pressurisation period. The bulk liquid's temperature initially remains at its saturation level since the tank is closed and pressure starts to increase. As a result, more evaporation takes place in comparison to the continuous self-pressurization duration.

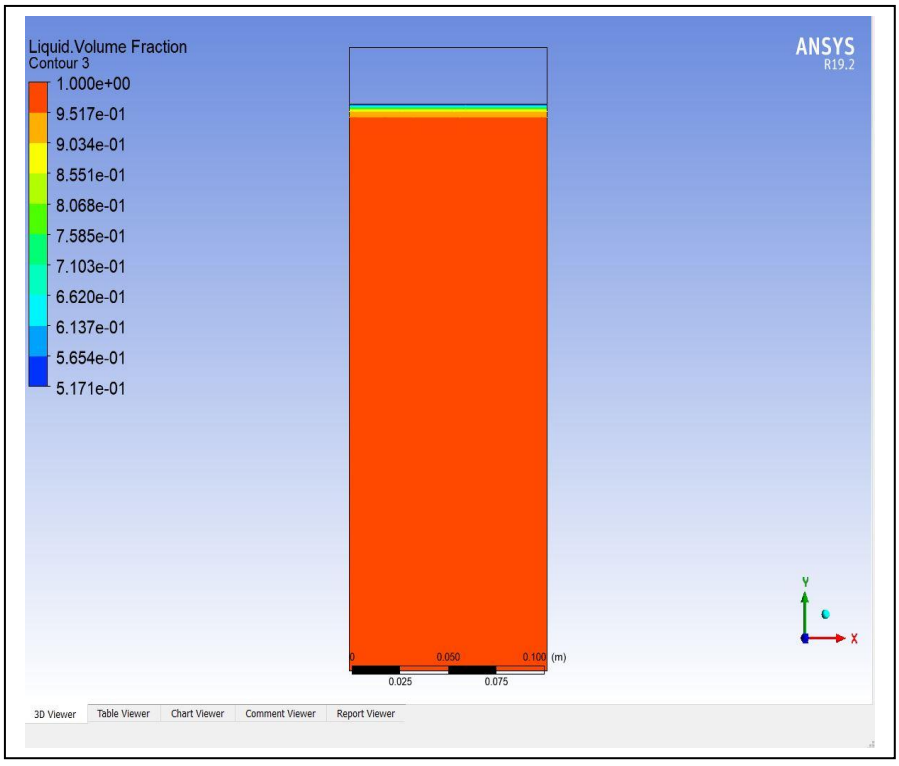

Fig 6.4: Volume fraction

The formation of the stratified layer has been thoroughly described by the numerical simulation. It is obvious that the liquid along the wall warms up and moves toward the interface as a result of the sidewall heating. This heated liquid that is depositing at the liquid-vapor interface is referred to as a thermally stratified layer. As we can observe, the temperature rises toward the interface from 79.791 K to 80.021 K.

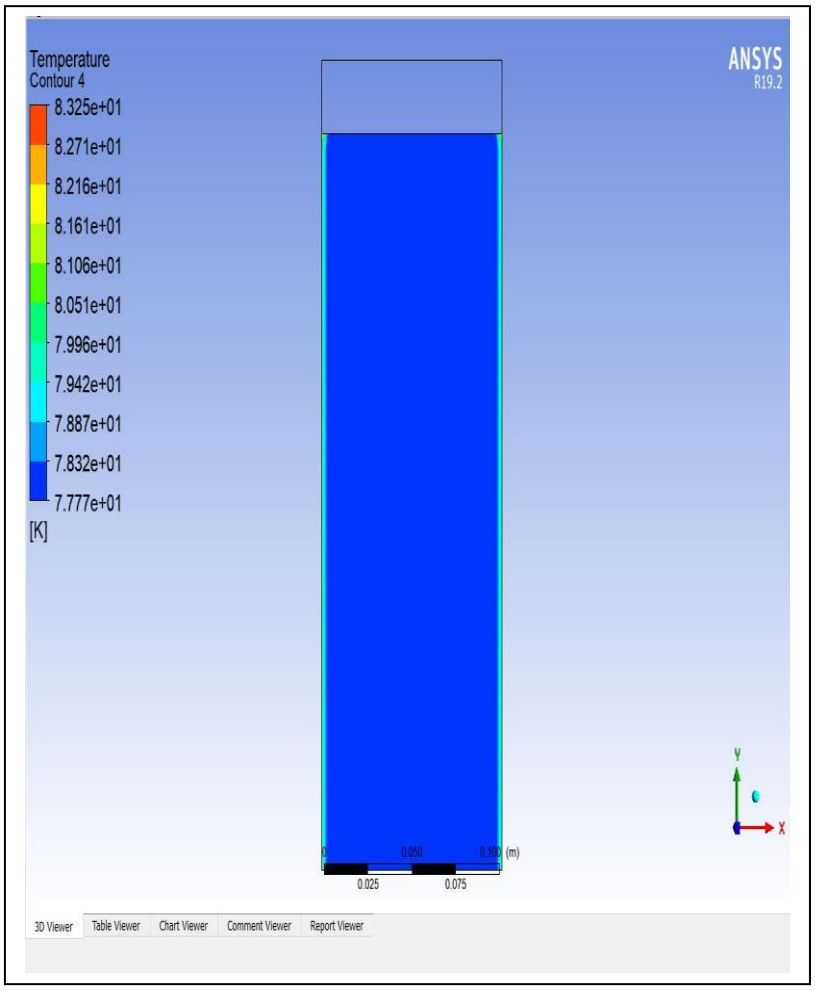

Fig 6.5: Evolution of stratification

The figure displays the evolution of the liquid's internal temperature over time. At each time point, a distinct stratified layer may be seen. From 79.942 K to 80.060 K, the temperature at the interface increases over time. The increase in stratum thickness parallels the deepening of the red zone.

6.3.2 Evolution of Pressure

Pressure rises virtually continuously in a microgravity environment. This is due to the phase transition that is occurring inside the tank. Since there is a continuous heat flux throughout, more liquid boils and the pressure rises. The stratification process will be facilitated by the higher fluid velocity and turbulent nature of the flow. However, after stratification, it seems as though the pressure value is declining and almost staying constant. It results from the fluid turbulence and the efficient mixing of the stratum layer and the bulk fluid. Although the bulk temperature will always be high in these conditions.

CHAPTER 7

CONCLUSIONS

This section emphasises the findings from the experimental, and numerical simulations. It also considers an extensive overview of the scope of ongoing activity based on completed work. An analytical model is developed utilising the correlations that are currently available and examines the effect of venting on the development of stratification. The model is validated using the results of experiments. The formation of stratification inside a cryogenic storage tank may be completely understood by conducting ground experiments. As part of an experimental setup, a specifically made high-pressure test tank with foam insulation has been designed and built for this. Liquid nitrogen is used as the cryogen.

The 2.2-liter test tank used in this experiment can hold liquid cryogens like nitrogen at design pressures as high as 4 bar absolute. Throughout the venting off period, stratification was being tested. A numerical model is developed to understand the fluidic and thermodynamic processes taking place inside a propellant tank. The results were validated by experiments. Using the developed computational model, a detailed analysis has been done to reduce stratification on a cylindrical storage tank.

7.1 CONCLUSIONS OF STUDY

- When compared to a venting scenario, the aftermath of the non-venting condition turns out to be entirely different.
- There is no discernible heat stratification when there is no venting. The temperature increase is merely a few decimal places.
- A significant temperature gradient appears along the height of the tank during non-venting condition.
- The rise in kinematic viscosity at higher operating pressures causes an increase in thermal stratification.
- The self-pressurization rate is directly influenced by the axial heat flux, demonstrating the need for improved insulation in cryogenic storage tanks.

7.2 SCOPE FOR FUTURE WORK

- It is feasible to optimise the propellant tank design and insulation thickness by taking into account additional elements, such as an increase in insulation mass with higher insulation thickness and condensation or ice development over the tank with lower insulation thickness.
- Improve the numerical model by incorporating 3D models.
- Although a steady heat flux is employed throughout the inquiry, aerodynamic heating and altitude fluctuation will cause differences in real-world conditions.

REFERENCES

A CFD simulation study of boiling mechanism and BOG generation in a full-scale LNG storage tank Abdullah Saleem , Shamsuzzaman Farooq , Iftekhar A. Karimi , Raja Banerjee**(2018).**

Barsi, S. and Kassemi, M., **(2008).** Numerical and experimental comparisons of the self-pressurization behavior of an LH2 tank in normal gravity. *Cryogenics*, *48*(3-4), pp.122-129.

Fu, J., Sunden, B. and Chen, X., **(2014)**. Influence of wall ribs on the thermal stratification and self-pressurization in a cryogenic liquid tank. *Applied Thermal Engineering*, *73*(2), pp.1421-1431.

Huerta, F. and Vesovic, V., **(2019).** A realistic vapour phase heat transfer model for the weathering of LNG stored in large tanks. *Energy*, *174*, pp.280-291.

Huerta, F. and Vesovic, V., **(2019).** Analytical solutions for the isobaric evaporation of pure cryogens in storage tanks. *International Journal of Heat and Mass Transfer*, *143*, p.118536.

Joseph, J., Agrawal, G., Agarwal, D.K., Pisharady, J.C. and Kumar, S.S., **(2017)**. Effect of insulation thickness on pressure evolution and thermal stratification in a cryogenic tank. *Applied Thermal Engineering*, *111*, pp.1629-1639.

Kang, M., Kim, J., You, H. and Chang, D., **(2018)**. Experimental investigation of thermal stratification in cryogenic tanks. *Experimental Thermal and Fluid Science*, *96*, pp.371-382.

Kang, M., Kim, J., You, H. and Chang, D., **(2018).** Experimental investigation of thermal stratification in cryogenic tanks. *Experimental Thermal and Fluid Science*, *96*, pp.371-382.

Kinefuchi, K., Kawashima, H., Sugimori, D., Umemura, Y., Okita, K., Kobayashi, H. and Himeno, T., **(2020)**. Experimental analysis of thermal behavior in cryogenic propellant tank with different pressurants. *Cryogenics*, *112*, p.103196.

Liu, Z. and Li, C., **(2018)**. Influence of slosh baffles on thermodynamic performance in liquid hydrogen tank. *Journal of hazardous materials*, *346*, pp.253-262.

Liu, Z., Li, Y. and Jin, Y., **(2016)**. Pressurization performance and temperature stratification in cryogenic final stage propellant tank. *Applied Thermal Engineering*, *106*, pp.211-220.

Numerical analysis of convective flow and thermal stratification in a cryogenic storage tank Sung Woong Choi, Woo Il Lee & Han Sang Kim**(2017).**

Ovidi, F., Pagni, E., Landucci, G. and Galletti, C., **(2019)**. Numerical study of pressure build-up in vertical tanks for cryogenic flammables storage. *Applied Thermal Engineering*, *161*, p.114079.

Ren, J.J., Shi, J.Y., Liu, P., Bi, M.S. and Jia, K., **(2013)**. Simulation on thermal stratification and de-stratification in liquefied gas tanks. *International journal of hydrogen energy*, *38*(10), pp.4017-4023.

Roh, S., Son, G., Song, G. and Bae, J., **(2013)**. Numerical study of transient natural convection in a pressurized LNG storage tank. *Applied Thermal Engineering*, *52*(1), pp.209-220.

Xavier, M., Raj, R.E. and Narayanan, V., **(2017)**, February. Thermal stratification in LH2 tank of cryogenic propulsion stage tested in ISRO facility. In *IOP conference Series: Materials Science and Engineering* (Vol. 171, No. 1, p. 012063). IOP Publishing.